UserCom

11

Dear Customer,

The year 2000 should prove to be extremely interesting for METTLER TOLEDO thermal analysis. We plan to expand the very successful **STA**R^e product line with the introduction of an exciting new instrument for dynamic mechanical analysis.
And of course the current thermal analysis instruments have been undergoing continuous development. In this edition of UserCom, we are delighted to present the new DSC822^e.

Interpreting DSC curves
Part 1: Dynamic measurements

The art of interpreting curves has yet to be integrated into commercially available computer programs. The interpretation of a DSC measurement curve is therefore still something you have to do yourself. It requires a considerable amount of experience in thermal analysis as well as a knowledge of the possible reactions that your particular sample can undergo.
This article presents tips and information that should help you with the systematic interpretation of DSC curves.

Recognizing artifacts

The first thing to do is to examine the curve for any obvious artifacts that could lead to a possible misinterpretation of the results. Artifacts are effects that are not caused by the sample under investigation. Figure 1 shows examples of a number of such artifacts. They include:

a) An abrupt change of the heat transfer between the sample and the pan:
   1) Samples of irregular form can topple over in the pan.
   2) Polymer films that have not been pressed against the base of the pan first change shape (no longer lie flat) on initial warming. Afterward, on melting, they make good contact with the pan (Fig. 2).

b) An abrupt change of the heat transfer between the pan and the DSC sensor:
   1) Distortion of a hermetically sealed Al pan due to the vapor pressure of the sample.
   2) Slight shift of the Al pan during a dynamic temperature program due to different coefficients of expansion (Al: ~ 24 ppm/K, DSC sensor ~ 9 ppm/K, see also Fig. 2). This artifact does not occur with Pt pans (~ 8 ppm/K).
   3) The measuring cell suffers a mechanical shock: The pans jump around on the sensor and can move sideways if they do not have a central locating pin.

Contents

c) The entry of cool air into the measuring cell due to a poorly adjusted measuring cell lid leads to temperature fluctuations which cause a very noisy signal.

d) Electrical effects:
   1) Discharge of static electricity in a metallic part of the system, or power supply disturbances (spikes)
   2) Radio emitters, mobile (cellular) phones and other sources of high frequency interference.

e) A sudden change of room temperature, e.g. through sunshine.

f) The lid of the pan bursts as a result of increasing vapor pressure of the sample. This produces an endothermic peak with a height of 0.1 mW to 100 mW depending on the quantity of gas or vapor evolved.

g) Intermittent (often periodic) closing of the hole in the lid of the pan due to droplets that condense or to samples that foam.

h) Contamination of the sensors caused by residues of a sample from previous experiments. The thermal effects characteristic for this substance always occur at the same temperature. This problem can often be overcome by heating the system in air or oxygen. This type of artifact is very dependent on the contaminant. Artifacts caused by pans that are not inert also look very similar. Figure 3 shows an example of this.

Artifacts can also interfere with automatic evaluations (with EvalMacro), especially those using automatic limits.
Isolated artifacts that have been definitely identified as such can be eliminated from the measurement curve using TA/Baseline.

Measurement conditions

You define the temperature range and the heating rate for the measurement based on your knowledge of the physical and chemical properties of the sample.

- Choose a temperature range that is on the large side. At a heating rate of 20 K/min, you do not in fact lose too much time if the range measured is 100 K too large. Further information on this can be found in UserCom 3.
- Use a sample weight of about 5 mg for the first measurement. Make a note of the total weight of the sample and pan so that you can detect a loss of weight by
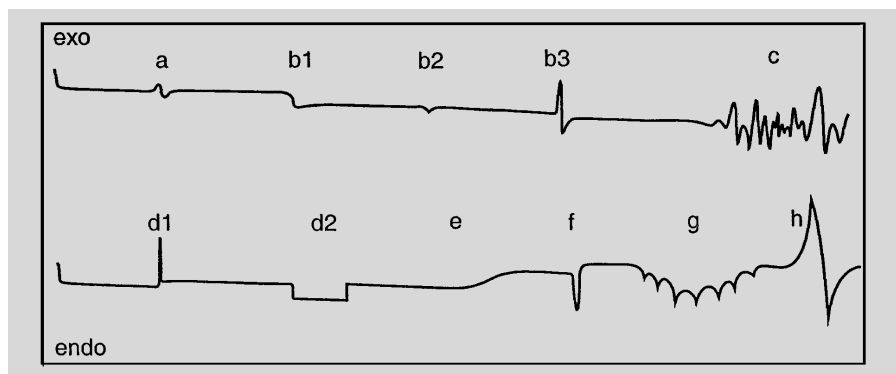

Fig. 1. DSC artifacts (details are given in the text): An artifact can very often be identified by repeating the measurement with a new sample of the same substance and observing whether the effect occurs again either at the same place or at a different place on the curve. Exceptions to this are f and h, which can be very reproducible.
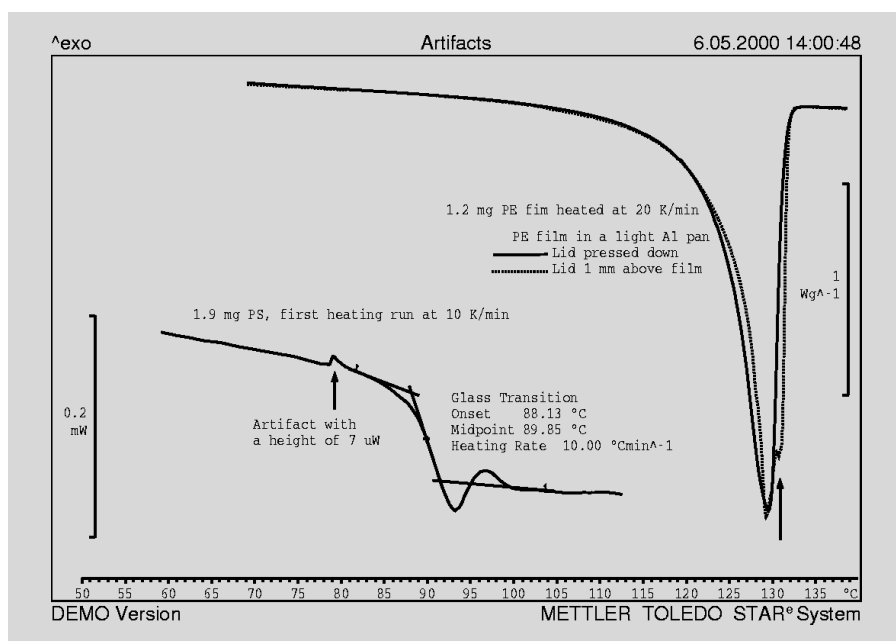

Fig. 2. Above: Artifact due to a PE film that was not pressed down firmly in the pan (dotted line). The sample of film that was pressed down on the base of the pan with the lid of a light Al pan gave the "correct" melting curve.
Below: DSC heating curve of 1.92 mg polystyrene showing a typical artifact at about 78 °C caused by the thermal expansion of the Al pan. This artifact, which is of the order of 10 μW, is only visible with large scale expansion (ordinate scale < 1mW).

reweighing after the analysis. The first measurement is often performed using a pan with a pierced lid and nitrogen as a purge gas.

- The first heating curve is usually measured from room temperature to the desired final temperature at a heating rate of 20 K/min.
- Interpretation is often facilitated by measuring a cooling curve directly afterward. The cooling rate that can be used depends on the cooling option installed in your system.
- It is a good idea to heat the sample a second time. Differences between the first and the second heating curves can be very informative.
- Another helpful variation is to shock cool the sample after it has been heated

for the first time to the final temperature. This freezes any possible metastable states. The sample is then measured a second time. A very convenient way to shock cool the sample to room temperature is to use the automatic sample robot. It deposits the hot sample on the cold aluminum turntable, which cools it down to room temperature within a few seconds. If you do not have a sample robot, you can wait until the sample has reached its final temperature and then remove the pan with tweezers and place it on a cold aluminum surface (with a 2 mm diameter hole for the pin) or immerse it for about 10 seconds in liquid nitrogen.
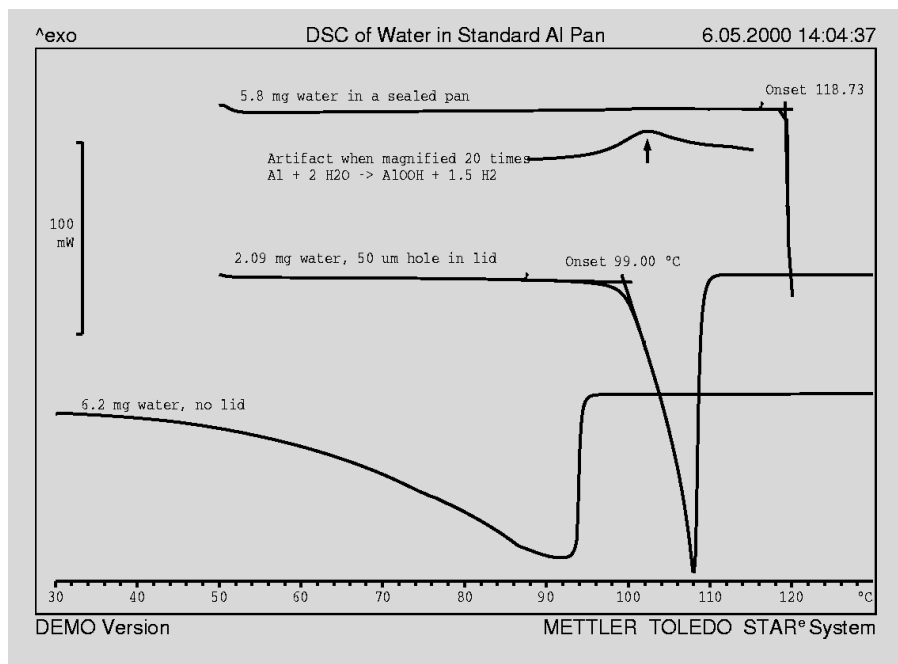
Fig. 3. Below: In an open pan, water evaporates before the boiling point is reached. Middle: In a self-generated atmosphere (50 μm hole in the lid), the boiling point can be measured as the onset. Above: In a hermetically sealed pan (at constant volume), there is no boiling point. The DSC curve is a straight line until the Al pan suddenly bursts at about 119 °C. If the ordinate scale is expanded 20 times, an exothermic peak can be observed that is due to the reaction of aluminum with water (see the expanded section of the curve).

If no thermal effects occur

In this case your sample is inert in the temperature range used for the measurement and you have only measured the (temperature dependent) heat capacity.

An inert sample does not undergo any loss of weight (except ≤30 μg surface moisture). After opening the pan, it looks exactly the same as before the measurement. This can be confirmed with the aid of a microscope for reflected light.

If you are interested in c_p values, you need a suitable blank curve. Check the plausibility of the results you obtain: values for c_p are usually in the range 0.1 to 5 $Jg^{-1}K^{-1}$.

To make absolutely sure that no effects occur, extend the temperature range of the measurement and measure larger samples.

If thermal effects are visible

Thermal effects are distinct deviations from the more or less straight line DSC curve. They are caused by the sample undergoing physical transitions or chemical reactions. If two effects overlap, try to separate them by using faster or slower heating rates, and smaller sample weights. Here, one should take into account that faster heating rates cause a marked shift in the peak maxima of chemical reactions to higher temperatures. To a lesser extent, this also applies to

solid-solid transitions and glass transitions. The onset temperatures of the melting processes of nonpolymeric substances are, however, independent of the heating rate.

If several effects occur with significant loss of weight (>30 μg), you would of course like to assign the latter to a particular peak - weight loss is usually an endothermic effect due to the work of expansion resulting from the formation of gas. One method is to heat a new sample step by step through the individual peaks and determine the weight of the pan and contents at each stage (at METTLER TOLEDO we call this "off-line thermogravimetry"). The best way is to measure a new sample in a TGA, ands use the same type of pan as for the DSC measurement.

The shape of the DSC curve is usually very characteristic and helps to identify the nature of the effect.

In the following sections, examples of the most important effects and their typical curve shapes will be discussed.

Physical transitions

Physical transitions can in principle be measured as many times as desired if
- on cooling, the sample reverts to the same state as before the transition. This, however, is not always the case and

depends on the sample and the cooling rate. Many substances in fact solidify from the melt at fast cooling rates to a glassy amorphous state. This is the reason why no melting peak occurs on heating the same sample a second time. Some metastable crystal modifications crystallize only in the presence of certain solvents.
- the sample does not escape from the pan through evaporation, sublimation, or (chemical) decomposition , or does not undergo transformation. Any sample lost by evaporation cannot of course condense in the sample pan on cooling because the purge gas has already removed it from the measuring cell .

Melting, crystallization and mesophase transitions

The heat of fusion and the melting point can be determined from the melting curve. With pure substances, where the low temperature side of the melting peak is almost a straight line (Fig. 4a), the melting point corresponds to the onset. Impure and polymeric samples, whose melting curves are concave in shape, are characterized by the temperatures of their peak maxima (Fig. 4b and c). Partially crystalline polymers give rise to very broad melting peaks because of the size distribution of the crystallites (Fig. 4c).

Many organic compounds melt with decomposition (exothermic or endothermic, Figs. 4d and 4e).

An endothermic peak in a DSC heating curve is a melting peak if
- the sample weight does not decrease significantly over the course of the peak. A number of substances exhibit a marked degree of sublimation around the melting temperature. If hermetically sealed pans are used, the DSC curve is not affected by sublimation and evaporation.
- the sample appears to have visibly melted after the measurement. Powdery organic substances, in particular, form a melt that on cooling either solidifies to a glass (with no exothermic crystallization peak) or crystallizes with an exothermic peak.

Comment: Many metals have a high melting point oxide layer on their surface. After melting, the oxide layer remains behind as a rigid envelope. This

is the reason why, on opening the pan, the sample looks exactly the same as before melting - it would in fact require samples weighing several grams to deform the oxide layer under the force of gravity, so that the sample fits the shape of the pan. Precious metals have no oxide layer and form spherical droplets on melting.

- its surface area is between about 10 Jg^{-1} and 400 Jg^{-1}. The heat of fusion on nonpolymeric organic substances is almost always between 120 Jg^{-1} and 170 Jg^{-1}.
- its width at half height (half-width) is significantly less than 10 K (partially crystalline polymers can melt over a wider range). The melting peak is increasingly sharper, the purer the substance and the smaller the size of the sample. Very small quantities of pure substances give peaks with half-widths of less than 1 K.

Impure samples and mixtures often show several peaks. Substances with eutectic impurities exhibit two peaks (Fig. 4b): first the eutectic peak, whose size is proportional to the amount of impurity, and then the main melting peak. Sometimes the eutectic is amorphous so the first peak is missing. Liquid crystals remain anisotropic even after the melting peak. The melt does not become isotropic until one or more small sharp peaks of mesophase transitions have occurred (Fig. 4f).

An exothermic peak on a cooling curve is a crystallization peak if

- the peak area is about the same as the melting peak - since the heat of fusion is temperature dependent, a difference of up to 20% can arise depending on the degree of supercooling.
- the degree of supercooling (the difference between the onset temperatures of melting and crystallization) is between 1 K and about 50 K. Substances that crystallize rapidly show an almost vertical line after nucleation until (if the sample is large enough) the melting temperature is reached (Figs. 5a, 5g).

If the liquid phase consists of a number of individual droplets, the degree of supercooling of each droplet is different so that several peaks are observed (Fig. 5b). Organic and other "poorly crystallizing" compounds form a solid glass on cooling
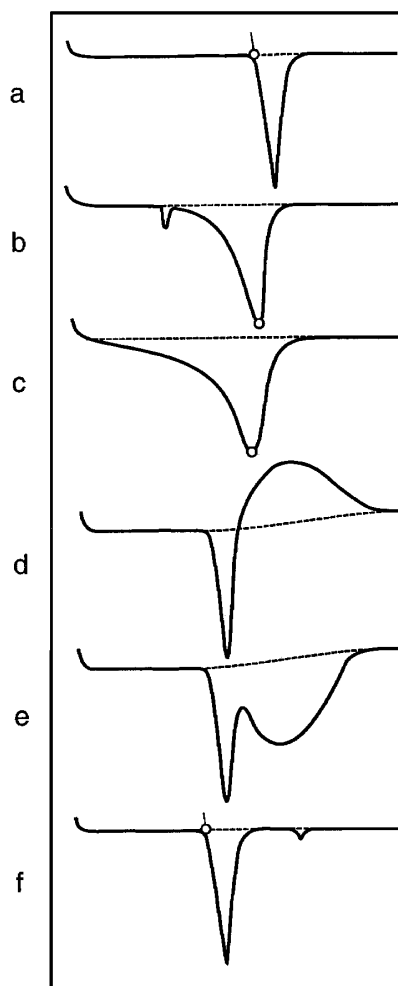

Fig. 4. Melting processes: a: a nonpolymeric pure substance; b: a sample wit a eutectic impurity; c: a partially crystalline polymer; d and e: melting with decomposition; f: a liquid crystal.

(Fig. 5c). Such amorphous samples can then crystallize on heating to temperatures above the glass transition temperature (devitrification, cold crystallization). Cold crystallization can often occur in two steps. On further heating, polymorphic transitions can occur before the solid phase finally melts (Fig. 5e).

When the melt of a sample containing eutectic impurities is cooled, the main component often crystallizes out (Fig. 5d). It can, however, solidify to a glass (Fig. 5c). Very often the eutectic remains amorphous so that the eutectic peak is missing.

A polymer melt crystallizes after supercooling by about 30 K (Fig. 5f). Many polymers solidify to glasses on rapid cooling (Fig. 5c).

When the melt of a liquid crystal is cooled, the mesophase transitions occur first (often without any supercooling). The subsequent crystallization exhibits the usual supercooling (Fig. 5g).
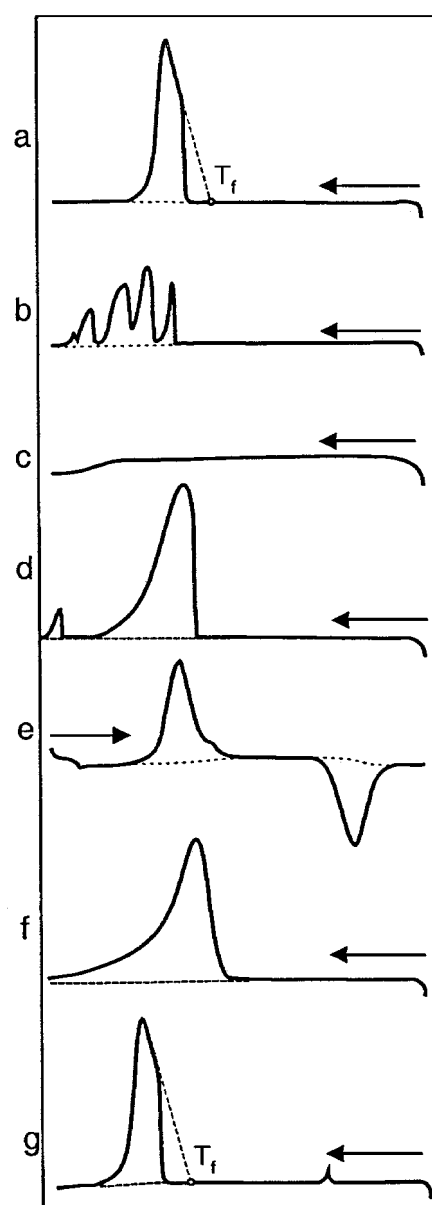

Fig. 5. Crystallization: a: a pure substance (T$_f$ is the melting point); b: separate droplets solidify with individual degrees of supercooling; c: a melt that solidifies amorphously; d: a sample with a eutectic impurity; e: a shock-cooled melt crystallizes on warming above the glass transition temperature (cold crystallization); f: a partially crystalline polymer; g: a liquid crystal

Solid-solid transitions, polymorphism

Solid-solid transitions can be identified by the fact that a sample in powder form is still a powder even after the transition. The monotropic solid-solid transition of metastable crystals (marked α' in Fig. 6) to the stable α-form, which is frequently observed in organic compounds, is exothermic (Fig. 6a). As the name implies, monotropic transitions go in one direction only (they are irreversible).

The monotropic transition is slow and is most rapid a few degrees K below the melt-

ing point of the metastable phase. In spite of this, the peak height is usually less than 0.5 mW and can therefore easily be overlooked alongside the following melting peak of about 10 mW (gray arrow in Fig. 6b). It is often best to measure the
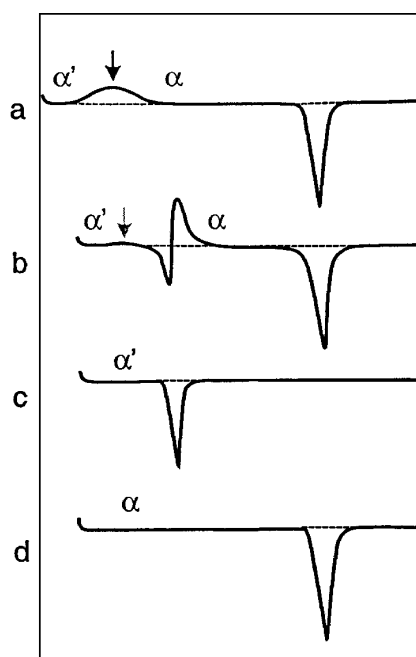

Fig. 6. Monotropic transition: a: the arrow marks the solid-solid transition, afterward the α-modification just formed melts; b: in this case the solid-solid transition is so slow that α crystallizes; c: the pure α'-form melts low; d: the pure α-form melts high.

monotropic transition isothermally.

At heating rates greater than 5 K/min, it is easy to "run over" the slow transition (Fig. 6b) and so reach the melting temperature of the metastable form. The monotropic solid-solid transition is either not visible or it could be falsely interpreted as a slightly exothermic "baseline shift" before the melting peak. If some stable crystals are present that can serve as nuclei for the crystallization of the liquid phase formed, the melting peak merges directly into the exothermic crystallization peak. This case is referred to as a transition via the liquid phase - on immediate cooling to room temperature, the sample would have visibly melted. Finally the melting temperature of the stable modification is reached.

If no α-nuclei are present, there is no α-crystallization peak and of course no α-melting peak (Fig. 6c). If the sample consists entirely of the stable form, then only the α-melting peak appears and the polymorphic effect is not observed (Fig. 6d). Depending on the substance, the α-form

melts at temperatures that are 1 K to 40 K lower than the stable modification.
The **enantiotropic solid-solid transition, which occurs** less often, is reversible. The α→β transition, starting from the low temperature form α to the high
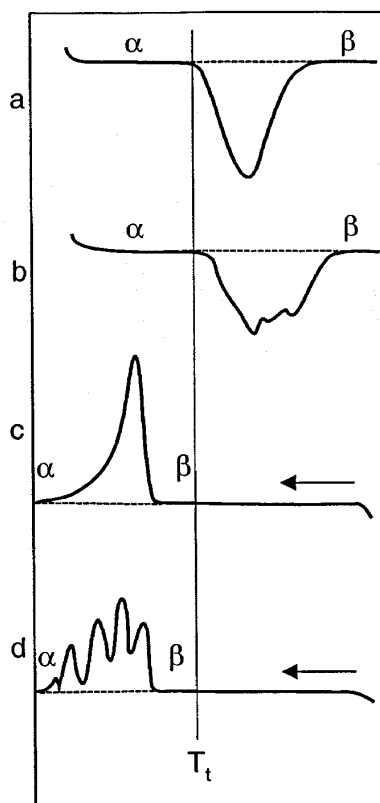

Fig. 7. Reversible enantiotropic transition: a: α fine powder; b: coarse crystals; c: reverse transition of the fine powder; d: reverse transition of the coarse crystals; at T_t, α and β are in thermodynamic equilibrium.

temperature form β is endothermic. The enantiotropic transition gives rise to peaks of different shape depending on the particle size of the sample because the nucleation rate of each crystal is different. For statistical reasons, samples that are finely crystalline give rise to bell-shaped (Gaussian) peaks (Figs. 7a and 7c). A small number of larger crystals can give rise to peaks with very bizarre shapes . This is especially the case for the reverse β→α transition (Figs. 7b and 7d).
The peaks of enantiotropic transitions typically have α half-width of 10 K.

Transitions with a distinct loss of weight

These types of transitions can of course only be observed in open pans, i.e. either a pan with no lid, or a pan with a lid and a 1 mm hole to protect the measuring cell from substances that creep out or that splutter.

Examples are:
- the evaporation of liquid samples (Fig. 3, below and Fig. 8a),
- drying (desorbtion of adsorbed moisture or solvents, Fig. 8b),
- the sublimation of solid samples (Fig. 8b) and the
- decomposition of hydrates (or solvates) with the elimination of the water of crystallization. In an open crucible, the shape of the curve corresponds that shown in Fig. 8b, and in a self-generated atmosphere to that in Fig. 8c.

These peaks have a half-width of ≥20 K (except in a self-generated atmosphere) and have a shape similar to that exhibited by chemical reactions. The decomposition of solvates is known as pseudo-polymorphism (probably because in a hermetically sealed pan, a new melting point occurs when the sample melts in its own water of crystallization) and can also be regarded as a chemical reaction.

In a self-generated atmosphere (with a 50 μm hole in the lid of the pan), the evaporation of liquids is severely hindered. The usual very sharp boiling peak (Fig. 3, middle and Fig. 8d) does not occur until the boiling point is reached.

Apart from the appreciable loss of weight, these reactions have another feature in common, namely that the baseline shifts in the exothermic direction due to the decreasing heat capacity of the sample.

The glass transition

At the glass transition of amorphous substances, the specific heat increases by about 0.1 to 0.5 $Jg^{-1}K^{-1}$. This is the reason why the DSC curve shows a characteristic shift in the endothermic direction (Fig. 2, below and Fig. 9a). Typically
- the radius of curvature at the onset is significantly greater than at the endset and
- before the transition, the slope is clearly endothermic, and after the transition the curve is (almost) horizontal.

The first measurement of a sample that has been stored for a long time below the glass transition temperature, T_g, often exhibits an endothermic relaxation peak with an area of 1 Jg^{-1} to a maximum of about 10 Jg^{-1} (Fig. 9b). This peak can no longer be observed on cooling (Fig. 9c), or on heating a second time. The glass transition covers a temperature range of 10 K to about 30 K.
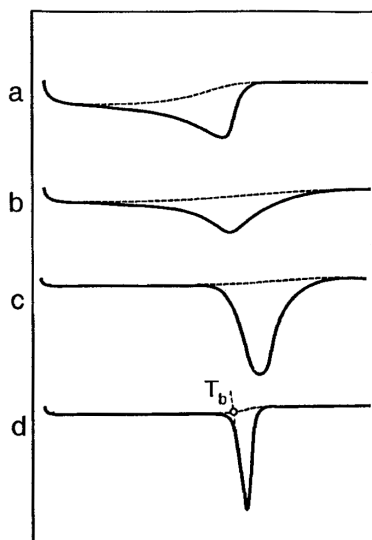
Fig. 8. Transitions with weight loss: a: evaporation in an open pan; b: desorbtion, sublimation; c: dehydration; d: boiling in a pan with a small hole in the lid, T_b is the boiling point.

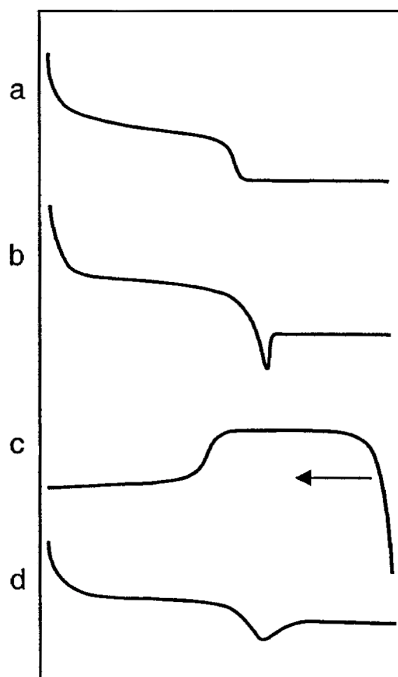**Fig. 9. Step transitions: a: a glass transition; b: a glass transition with enthalpy relaxation; c: the reverse transition; d: a Curie transition**
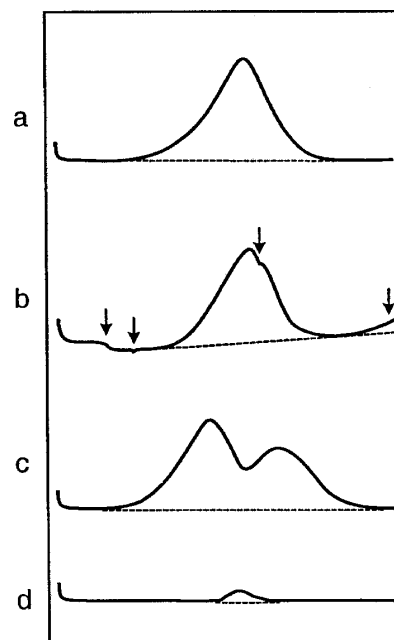

Fig 10. Curve shapes of chemical reactions: a: an ideal exothermic reaction; b: reaction with "interfering" physical transitions and the beginning of decomposition; c: chemical reaction with a secondary reaction; d: partial oxidation of organic samples with the residual oxygen in a hermetically sealed pan.

You can identify an effect that resembles a glass transition by checking whether the sample is visibly soft, almost liquid or rubbery-like above the T_g. If you do not have access to a TMA or DMA instrument, you can check this by heating a sample up to a temperature of T_g + 20 K in a pan without a lid. After several minutes at this temperature, you open the lid of the measuring cell and press the sample with a spatula or a needle. It is, however, difficult to detect softening in this way especially with polymers containing large amounts of fillers.

Lambda transitions

These types of solid-solid transitions exhibit Λ-shaped c_p temperature functions. The most important is the ferromagnetic Curie transition, which was previously used to calibrate the temperature scale of TGA instruments. The DSC effect is however extremely weak (Fig. 9d). To make sure, you can check that the sample is no longer magnetic above the Curie temperature with a small magnet.

Chemical reactions

Chemical reactions can in general only be measured in the first heating run. On cooling to the starting temperature, the reaction product remains chemically stable, so that on heating a second time no further reaction takes place [1]. In some cases, however, the reaction does not go to completion during the first heating run, so that on heating a second time, a weak postreaction can be observed (e.g. the curing of epoxy resins).

The half-width of chemical reaction peaks is about 10 K to 70 K (usually about 50 K at a heating rate of 10 K /min to 20 K/min). Reactions which show no significant loss of weight are usually exothermic (about 1 Jg^{-1} to 20 000 Jg^{-1}, Figs. 10a and 10b). The others tend to be endothermic because the work of expansion predominates.

Ideally, DSC curves of a chemical reaction show a single smooth peak (Fig. 10a). In practice, however, other effects and reactions often overlap and distort the peak shape, e.g. the melting of additives (Fig. 10b), or secondary or decomposition reactions (Fig. 10c).

Examples of reactions with significant loss of weight are:
- thermal decomposition (pyrolysis under an inert gas), with CO, short-chain alkanes, H_2O and N_2 as the most frequently occurring gaseous pyrolysis products,
- depolymerization with more or less quantitative formation of the monomer and
- polycondensation, for example the curing of phenol and melamine resins.[2]

Reactions with a significant increase of weight nearly always involve oxygen and are strongly exothermic. Examples are:
- the corrosion of metals such as iron and
- the initial uptake of oxygen at the beginning of the oxidation of organic compounds. During the course of the reaction, volatile oxidation products such as carbonic acids, CO_2 and H_2O are formed, so that finally a weight loss occurs (the initial increase in weight can be seen best in a TGA curve).

Examples of reactions with no significant change in weight are[3]:

- addition and polyaddition reactions, curing of epoxy resins,
- polymerizations, dimerizations,
- rearrangements and
- the oxidation of organic samples (e.g. polyethylene) with the residual atmospheric oxygen (about 10 μg) in a hermetically sealed pan (Fig. 10d).

Final comments

This article should help you to interpret DSC curves. You will, however, often have to use additional methods for confirmation. Some important techniques are:

- thermogravimetric analysis, ideally in combination with DTA or SDTA. The interpretation of DTA and SDTA® curves is analogous to DSC with limitations due to reduced sensitivity,
- thermomechanical and dynamic mechanical analysis,
- the analysis of the gaseous substances evolved (EGA, Evolved Gas Analysis) with MS or FTIR and
- the observation of the sample on a hot stage microscope (TOA, Thermo-Optical Analysis in the FP82 or the FP84 with simultaneous DSC)

In addition, various other chemical or physical methods are available. These depend on the type of sample, and can be applied after each thermal effect has taken place.

[1] There are very few exceptions to this rule; one example is the polymerization of sulfur, which begins on heating at about 150 °C and which is then reverted on cooling at about 130 °C.

[2] These slightly exothermic reactions are often measured in high pressure crucibles in order to suppress the endothermic vaporization peak of the volatile side-products.

[3] These reactions are often performed in hermetically sealed Al pans in order to prevent the release of small amounts of volatile components.

New in our sales program

DSC822[e]

Specifcations

Temperature range	-150 – 700 °C
Temperature accuracy	± 0.2 °C
Temperature reproducibility	± 0.1 °C
Sensor type	FRS5 ceramic sensor with 56 AuAuPd thermocouples
Signal time constant	2.3 s
Measurement range	700 mW
Digital resolution	16 million points
Sampling rate	Max. 10 points per second (selectable)

In the new DSC822[e], both the temperature and the DSC signal are measured with an analog to digital converter whose resolution is 16 times better than that used previously. This allows the temperature to be controlled more accurately and results in a marked reduction of the noise on the DSC signal (Fig. 1).

In the DSC821[e], the DSC signal range of 700 mW was defined by 1 million points, giving a resolution of 0.7 μW. In the new DSC822[e], this signal range is now defined by 16 million points and is therefore much more accurately resolved.

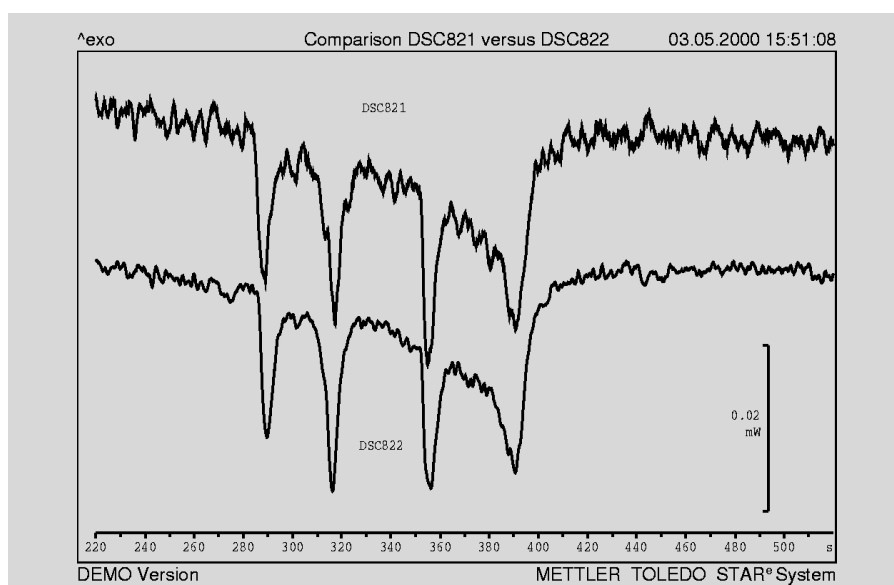Operation of the DSC822[e] requires the latest version of the **STAR**[e] software, V6.10.

Fig. 1. The above measurement of a liquid crystal demonstrates the improved signal to noise ratio.

Applications

The glass transition from the point of view of DSC measurements; Part 2: Information for the characterization of materials

Introduction

In the first part of this work (UserCom 10), the basic principles of the glass transition as well as its measurement and evaluation were discussed. This second part describes a number of practical aspects.

A glass transition always requires the presence of a certain degree of disorder in the molecular structure of the material under investigation (e.g. amorphous regions). It

content and consequently the intensity of the glass transition (step height Δcp) decrease.

The molecular mobility in amorphous regions is influenced by the presence of crystallites. This is particularly the case with polymers because some macromolecules are part of both the crystalline and the amorphous components. As a result of this, the glass transition is broader and is shifted

cause some of the amorphous regions cannot participate in the cooperative rearrangements. This rigid amorphous phase is located at the surface of the chain-folded crystals. This allows the proportion of the rigid amorphous material in polymers to be determined by measuring the step height as a function of the degree of crystallization.
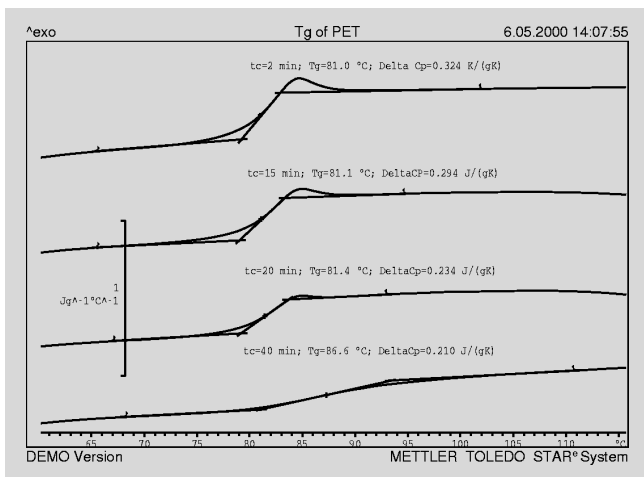

Fig. 1. The specific heat capacity of PET is shown as a function of temperature in the region of the glass transition. The sample was crystallized at 120 °C for different periods of time (tc). The crystallinity increases with the crystallization time, while Δcp (DeltaCp) decreases. (Sample weight: 14 mg, heating rate: 10 K/min).
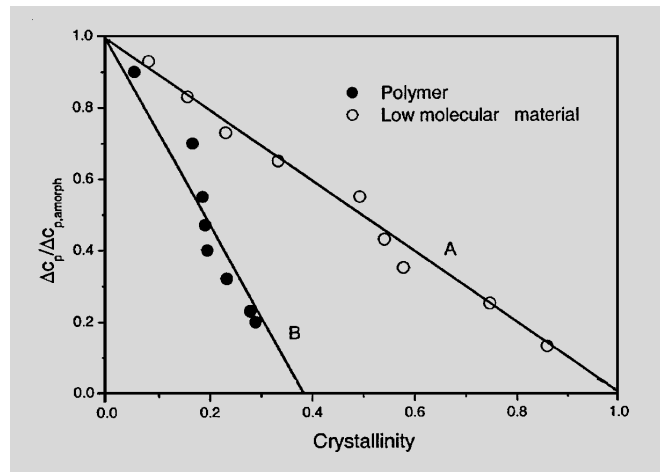

Fig. 2. The normalized step height of the specific heat at the glass transition as a function of the crystallinity. (Polymer: PET crystallized isothermally at 120 °C), A: Behavior of a two phase system; B: Measured behavior for a three phase system.

is very sensitive to changes in molecular interactions. Measurement of the glass transition can therefore be used to determine and characterize structural differences between samples or changes in materials. The following article presents a number of examples to illustrate the type of information that can be obtained from an analysis of the glass transition.

Partially crystalline materials

In addition to completely amorphous or completely crystalline materials, there are of course materials that are partially crystalline. In these types of material, crystallites and amorphous regions coexist. With increasing crystallinity, the amorphous

to higher temperature. This behavior is illustrated in the example in Figure 1, which shows the glass transition of various samples of polyethylene terephthalate (PET) that have been crystallized under different conditions. In Figure 2, the normalized step height at the glass transition is shown as a function of crystallinity for a number of different PET samples that had been allowed to crystallize for different periods of time at 120 °C. The line marked A represents a two phase behavior that can occur with low molecular weight substances in which only crystals and mobile amorphous material are present. Deviations from this behavior can occur with polymers due to the molecular size be-

Orientation

When thin films or fibers are manufactured from polymers, a molecular orientation is introduced that influences the glass transition. Analogous to the behavior of partially crystalline polymers, the glass transition temperature is shifted to somewhat higher temperatures and the glass transition itself becomes broader. Orientation (e.g. stretching) of partially crystalline polymers can increase the crystallinity to a marked degree. This effect can also be observed at the glass transition. Stretched polymers, however, very often shrink on heating. This changes the contact between the sample and the DSC sensor during the measurement. The shrinking process begins at the

glass transition and can result in DSC curves that are completely unusable. Only a preheated sample (a sample that has already shrunk) can be measured reproducibly. However, preheating the sample eliminates the thermal and mechanical history of the sample.

Figure 3 shows the glass transition of orientated PET fibers. The beginning of the glass transition is clearly visible in the first measurement. However, recrystallization already begins during the glass transition (exothermic peak between 80 °C and 140 °C). The fiber shrinks in this temperature range. If the fiber is heated to a temperature just below the melting temperature and then cooled, the sample is par-

The glass transition temperature was determined from these curves using two methods: firstly as the point at which the bisector of the angle between the two tangents intersects the measurement curve, (T_{g1}), and secondly as the "fictive temperature" according to Richardson's method, (T_{g2}). While T_{g1} increases with aging, T_{g2} decreases continuously. In addition, the enthalpy relaxation was evaluated according to the method described in Part 1 of this article. The results are shown in Figure 5. It can be clearly seen that the change of T_{g2} with time is analogous to that of enthalpy relaxation. T_{g2} describes the physical state of the glass before the measurement. The course of T_{g1} is however, also dependent on

If an epoxy resin is cured isothermally at a temperature of T_c, the glass transition temperature increases with increasing curing time. If the glass transition temperature of the cured material is greater than T_c, then vitrification occurs. The sample changes from a liquid to a glassy state. The reaction rate thereby decreases drastically and the glass transition temperature from then on changes only very slowly (see Fig. 8). At the vitrifications time, t_v, the glass transition temperature is equal to the curing temperature.

A similar relationship between the glass transition temperature and the degree of crosslinking (degree of vulcanization) can also be observed with many elastomers.
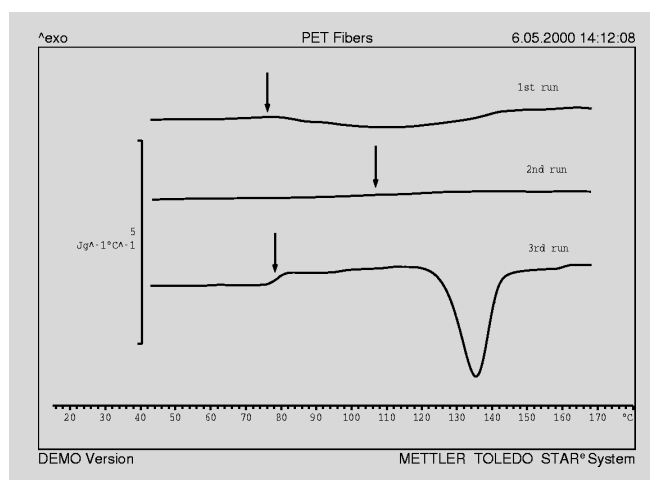

Fig. 3. Glass transition of stretched PET fibers (see text for details). The arrows mark the glass transition (Sample weight: 4 mg, heating rate: 10 K/min).

Fig. 4. Glass transition of samples of PET that have been stored for different periods of time at 65 °C. (Sample weight: 23 mg, heating rate: 10 K/min).

tially crystalline and shows a broad glass transition at a somewhat higher temperature (2nd run in Figure 3). If the fiber is melted and then shock cooled (3rd run), the sample is amorphous. The measurement curve shows the glass transition and the subsequent exothermic recrystallization peak.

Physical aging

As has already been discussed in Part 1 of this article (UserCom10), both the shape of the curve in the region of the glass transition and the glass transition itself depend on the actual storage conditions below the glass transition. Longer storage times lead to the formation of an enthalpy relaxation peak. This process is known as physical aging. To illustrate this effect , a series of heat capacity curves are shown in Fig. 4, using samples of polyethylene terephthalate (PET) that had been stored for different periods at 65 °C.

the actual measurement conditions. The enthalpy relaxation peaks are dependent on internal stresses that, for example, originate in the processing conditions, and depend on the thermal history during processing and storage. As can be seen in Fig. 6, these peaks can occur at different places in the glass transition region depending on the sample and the thermal history. The samples were cooled rapidly before performing the second measurement. This cooling process performed under defined conditions eliminated the effects of thermal history.

Crosslinking

In crosslinked systems (thermosets such as epoxy resins), the glass transition temperature is dependent on the degree of crosslinking. With increasing crosslinking, the glass transition shifts to higher temperatures (see Fig. 7).

However, the changes are relatively small (Fig. 9) because the density of crosslinking is relatively low.

Molar mass

In much the same way as a crosslinking reaction, the glass transition temperature in a polymerization increases with increasing molar mass M_w. The maximum value of T_g is reached at a molar mass of 10^4 to 10^5 g/mol. The relationship can be described to a good approximation (Fig.10) by the equation

$$T_g = T_{g\infty} - \frac{J}{M_w}$$

J is a polymer-specific constant.

Plasticizers

Figure 11 shows the effect of the plasticizer content on the glass transition of a polyvi-

nyl acetate (PVAc). Increasing concentrations of plasticizer cause the glass transition temperature to shift to lower values (Fig. 12). With some materials, it is possible for water (moisture) absorbed from the air to act as a plasticizer. Solvent residues, originating from the manufacture or processing of the material, can also behave as (unwelcome) plasticizers.

Polymer mixtures

Because of the large variety of polymer mixtures (polymer blends), only a few aspects of the glass transition can be mentioned here.
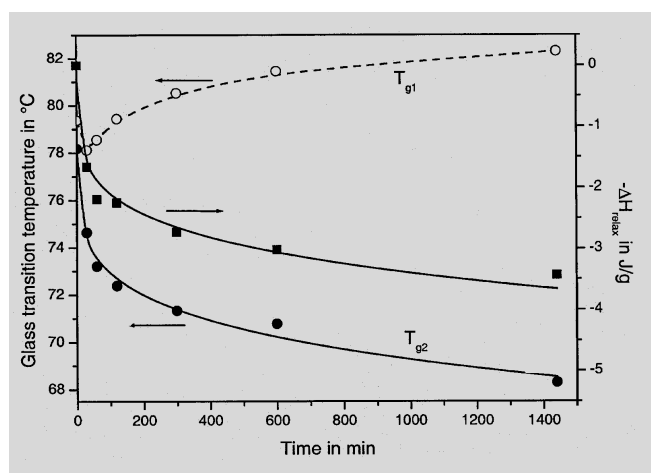
An example of an incompatible mixture is shown in Figure 13. A polycarbonate (PC) was mixed with ABS. The two glass transitions can be clearly seen in the measurement curve of the mixture. The PC glass transition temperature is lowered by about 3 K due to interaction with the ABS. From the ratio of the step heights of the PC glass transition ($\Delta cp_{pure}/\Delta cp_{mixture}$), it can be estimated that the mixture consists of 67% PC and 33% ABS.

With miscible substances, a homogeneous phase is formed and one single glass transition is measured. The glass transition temperature T_g depends on the concentra-

crease depending on which components were mixed together. In such cases, at least two glass transitions are observed after separation.

Copolymers

With copolymers, the glass transition is dependent on the type of polymerized monomers and their configuration in the macromolecule. If the monomers are miscible or statistically distributed, then one single glass transition is observed. With block and graft polymers, a phase separation often occurs. Two glass transitions are then measured. If the blocks are too short, then for chemical reasons no phase separation can
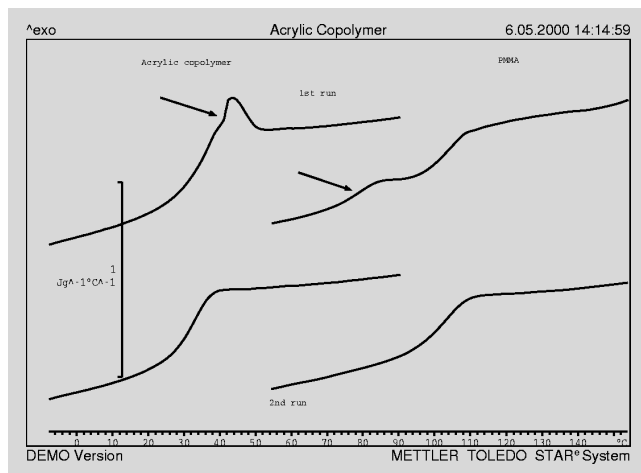
Fig. 5. Glass transition temperature T_{g1} (intercept of the bisector; open circles) and T_{g2} (according to Richardson; black dots) as well as the enthalpy relaxation -ΔH_{relax} of PET (aged at 65 °C) as a function of the aging time.

Fig. 6. First and second measurements of the glass transition of an acrylic copolymer and PMMA. The arrows mark the relaxation peaks.

In principle, polymers are either miscible (compatible) or immiscible (incompatible). With immiscible polymers, the individual components occur as separate phases. Regions of different phases exist at the same time alongside one another. Each of these phases can individually undergo a glass transition which means that several different glass transitions are measured. A comparison of the step heights and the glass transition temperatures with those of the pure components can provide information on the relative content of the phases and possible interactions between the phases, as well as on the quality of the mixing process. If the various glass transitions lie very close to each other, it is very difficult to separate them in a "normal" analysis. Annealing at a temperature just below T_g produces relaxation peaks that often allow a separation to be made.

tion of the individual components. The relationship between the glass transition temperature and the composition can be described by the semi empirical Gordon-Taylor equation:

$$T_g = \frac{w_1 T_{g1} + k w_2 T_{g2}}{w_1 + k w_2}$$

T_{g1} and T_{g2} are the glass transition temperatures of the pure components and w_1 and w_2 are the proportions by weight. k can be looked upon as being a fit parameter. The change of the glass temperature as a function of concentration of the concentration of PS-PPE blends is shown in Figure 14. (PPE is polyphenylene ether).

A homogeneous mixture need not necessarily be stable. A phase separation can occur as a result of a temperature increase or de-

take place, and only one transition is observed. Figure 15 shows the glass transitions of a gel consisting of two block copolymers. The substances differ only in the length of the blocks. In sample 2, the blocks are relatively long and a phase separation occurs. In sample 1, a phase separation is not possible because the blocks are short.

Chemical modification

Chemical modification can also influence molecular mobility. Phase separation is in this case also possible. Chemical modification can be deliberate or can occur through chemical aging. In chemical aging, degradation or oxidation takes place. An example of a deliberate modification is the chlorination of polyvinylchloride (PVC). Figure 16 shows the effect of the chlorine
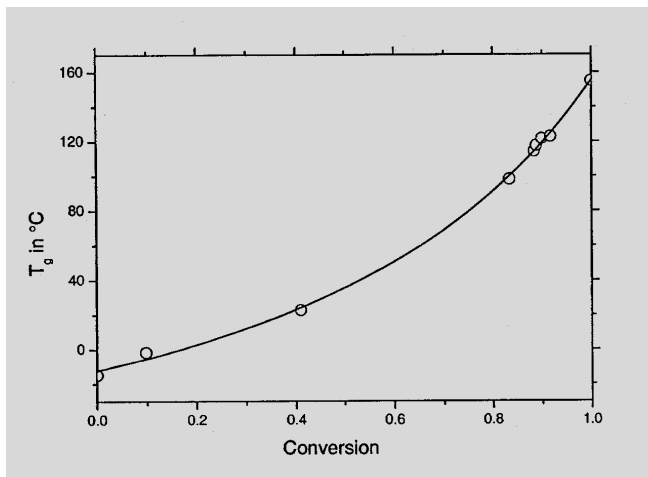
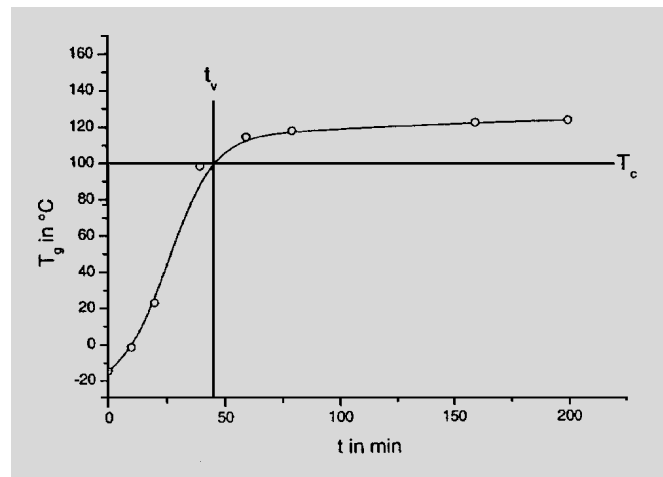Fig. 7. Glass transition temperature as a function of the degree of cross-linking of an epoxy resin system.

Fig. 8. Change of the glass transition temperature during the isothermal cross-linking of an epoxy resin system at $T_c = 100$ °C. New samples were cured for different periods of time at T_c and then cooled rapidly. The glass transition temperature was determined from the heating measurement at 10 K/min.
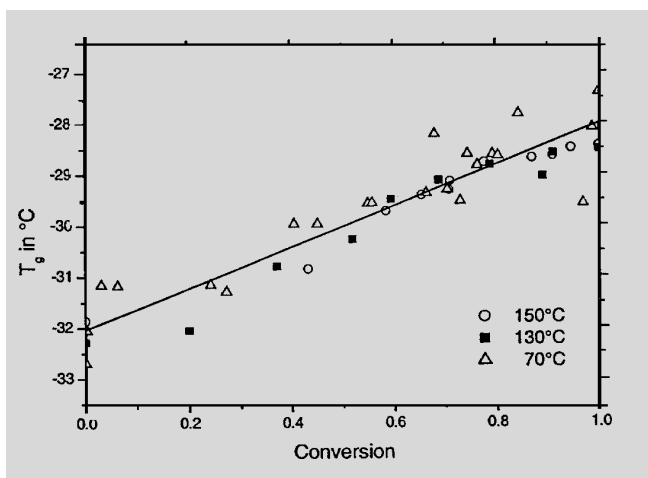

Fig. 9. Glass transition temperature as a function of the degree of vulcanization of an NBR rubber (Nitrile-Butadiene-Rubber). The samples were vulcanized isothermally at 70 °C, 130 °C and 150 °C.
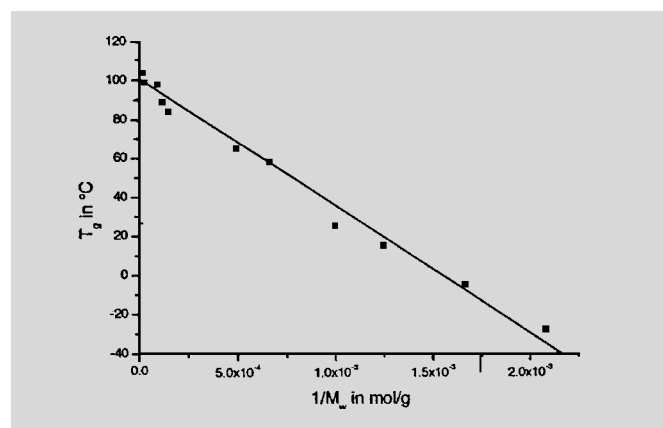
Fig. 10. Glass temperature of polystyrene (PS) as a function of the reciprocal mole mass (Tg∞ = 101 °C, J = 2.2 kgK/mol).

concentration on the glass transition. Higher concentrations of chlorine decrease the molecular mobility. As a result of this, the glass transition shifts to higher temperatures.

The broadening of the glass transition with increasing chlorine content is particularly noticeable. The reason for this is the relatively large degree of inhomogeneity of the chlorine distribution.

In chlorination, a hydrogen atom is replaced by a chlorine atom. This does not change the number of degrees of freedom of a monomer unit. The step height (Δcp) with respect to the mole therefore remains unaffected by chlorination. The reduction of the step height with increasing chlorina-

tion, which is apparent in Figure 16, is therefore due to the increase in size of the molar mass. This allows the change of Δcp to be used to estimate the chlorine content. The molar mass of a PVC monomer unit, MPVC, is 65.5 g/mol. Because the molar mass of chlorine is 35.5 g/mol, this gives a value of 56.8% for the chlorine content of PVC. The Δcp step height, Δc_{PVC} is 0.28 J/gK. This corresponds to 18.34 J/molK. The height of the Δcp step of the chlorinated PVC sample with the lower content of chlorine can determined relatively accurately (Δc_{PVCC}= 0.24 J/gK). The molar mass of the chlorinated PVC, M_{PVCC,} can be estimated from the equation

$$M_{PVCC} = M_{PVC} \frac{\Delta c_{PVC}}{\Delta c_{PVCC}}$$

In the case considered, this gives a value of M_{PVCC}=76.41 g/mol. This corresponds to 1.31 chlorine atoms per monomer unit and hence a chlorine content of 60.8%. This agrees very well with the data given for this sample.

Fillers

Inert substances such as glass fibers, chalk or carbon black are often added to polymers as fillers. They lower the polymer content of the materials and thereby reduce the step height of the glass transition. The step height Δc_p is proportional to the polymer content. In general, the glass transition temperature is independent of the filler content. Only with active fillers can relatively small changes in Tg be observed.

Conclusions

The glass transition is a phenomenon that can be observed in (partially) disordered systems as a step in the heat capacity curve. It is normally characterized by the glass transition temperature, T_g, the step height, Δc_p, and the width of the transition. Various methods can be used to determine the glass transition. The glass transition is primarily a result of molecular interactions and can therefore be used to detect small changes in the structure of samples.
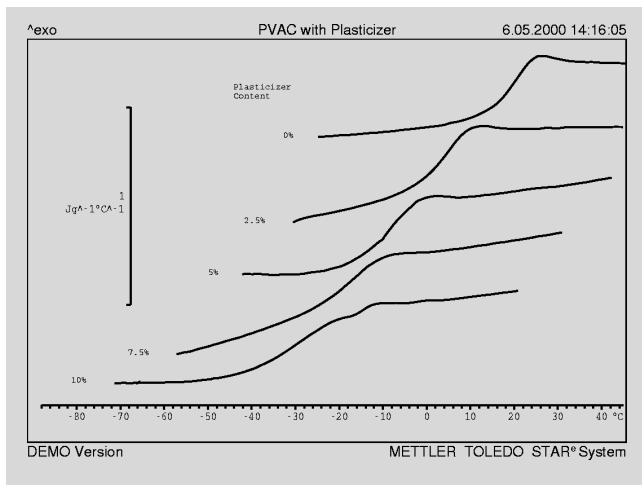
Fig. 11. Heat capacity as a function of temperature in the glass transition region of PVAc containing different concentrations of plasticizers.
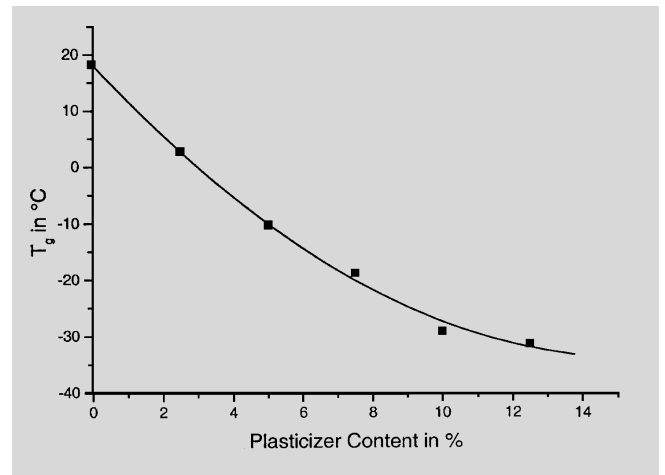
Fig. 12. Glass transition temperature of PVAc as a function of the plasticizer content (data from the measurements in Fig. 11).
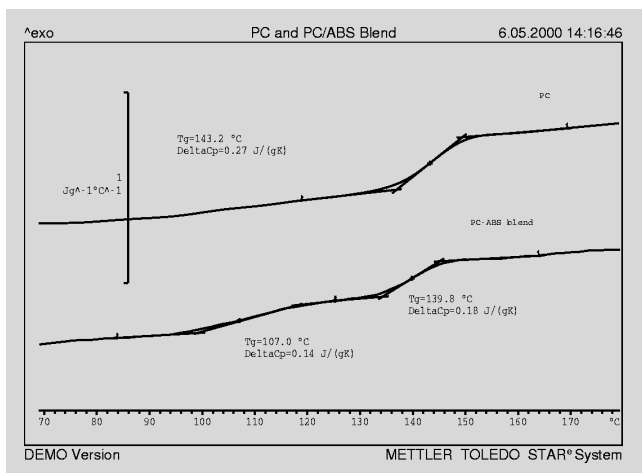
Fig. 13. Glass transition of samples of pure PC and a PC-ABS blend (sample weight about 10 mg, heating rate: 10 K/min).
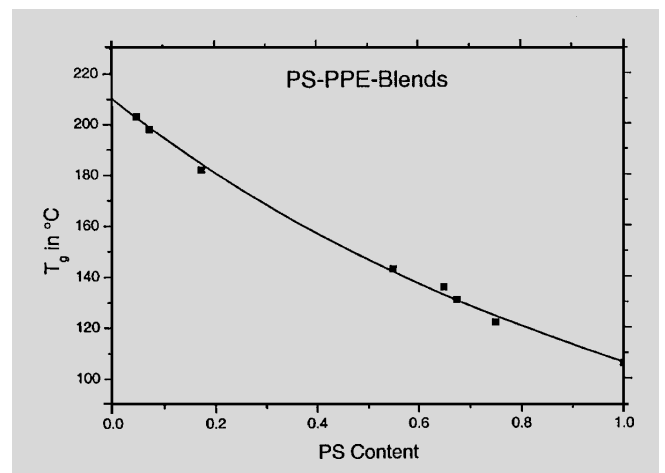
Fig. 14: Glass transition temperature as a function of the composition of PS-PPE mixtures. The continuous curve corresponds to the Gordon-Taylor equation with k = 0.63.
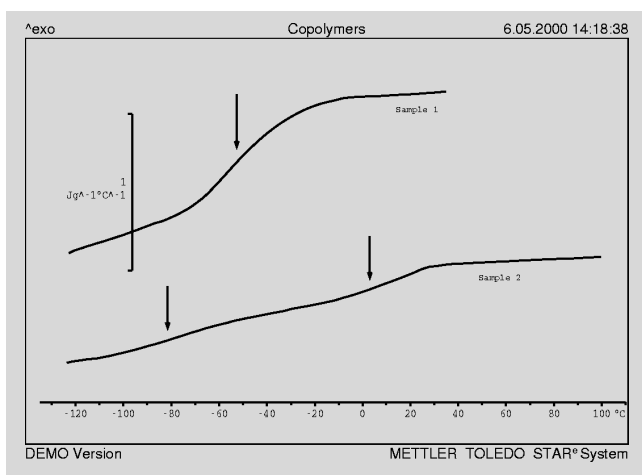
Fig. 15. Glass transition region of gels of block copolymers made of the same components but with different block lengths. The arrows mark the glass transitions (sample 1: short blocks; sample 2: long blocks).
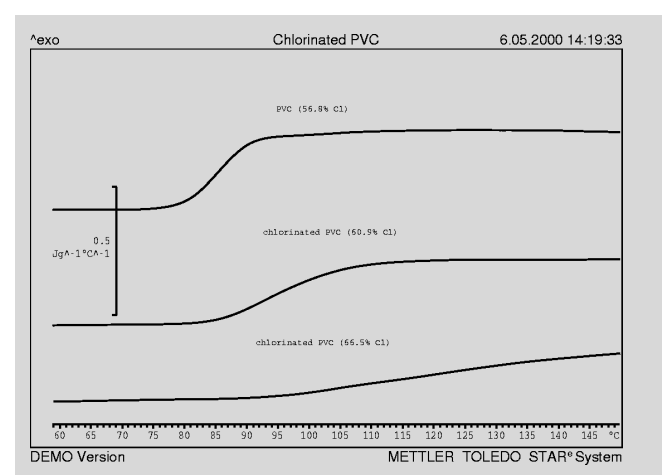
Fig. 16. Glass transition of samples of PVC and PVC that have been chlorinated to different extents. In the sample with 66.5% Cl, the glass transition is so broad that it has still not been completed at 150 °C.

One problem that affects the measurement and evaluation of the glass transition is the fact that the change in heat capacity can be very small (particularly with filled or partially crystalline materials). To improve the resolution, it is best to measure relatively large samples (e.g. with polymers typically 10 mg to 20 mg). In addition, thermal contact should be optimized, for example by compacting powders or by premelting in the pan. Usually a combination of measurements involving heating, cooling and then heating a second time yields the information required. The investigation can be supplemented by measuring samples that have been annealed just below the glass transition temperature. With these types of sample, both temperature-dependent and time-dependent peaks occur. Broad and flat transitions are particularly difficult to detect. In this case, subtraction of a blank curve often makes the evaluation easier. A major problem when determining the glass transition temperature is where to draw the tangents. A lot of care should be taken in the evaluation of the curve. It is essential to use adequate scale expansion for the relevant part of the curve. If several glass transition are to be compared with one another, it is best to normalize the curves with respect to sample weight or to evaluate the heat capacity. Furthermore it helps to display the curves in a coordinate system and to choose the tangents so that in all the curves the high and the low temperature tangents run parallel to each other. This allows even small changes in the glass transition temperature to be systematically detected and evaluated.

The glass transition temperature is not a thermodynamic fixed point . It depends on the heating and cooling rates, the thermal and mechanical history and the method used to determine it. Especially when large overheating peaks occur, Richardson's method (glass transition temperature as the fictive temperature) gives results for the glass transition temperature that are more significant and more reproducible than those from other methods. In any case, the step height should also be included in the evaluation, because this value contains important information about the material under investigation.

Summary		
Crystallinity	**Effect on the glass transition:** Increasing crystallinity $\rightarrow$ smaller step height; The glass transition is larger and broader.	**Special comments:** For low molecular substances, the crystallinity can be determined from Δc_p; for polymers the proportion of the T_g rigid amorphous phase
Crosslinking, curing, polymerization, molar mass	T_g shifts to higher temperature with increasing molar mass or crosslinking.	T_g bei M_w ab ca. 10^4 g/mol is c onstant
Orientation and storage below T$_g$	Internal stresses and storage shift T_g and increase the size of the enthalpy relaxation peak.	Possible crystallization in the glass transition region; Often, the first measurement cannot be used; Possibly use the evaluation, according to Richardson. The relaxation peaks contain information about the sample history.
Plasticizers	Plasticizers shift T_g to lower temperatures.	Solvent residues and moisture often behave as plasticizers (T_g is higher in the 2nd measurement if weight loss occurs)
Mixtures	Incompatible mixtures give two transitions, compatible mixtures only one.	The content can be determined from T_g as a function of the composition or the step height;
Copolymers	Block and graft copolymers of compatible monomers and statistical copolymers show one transition; otherwise two transitions.	T_g and the width of the transitions depend on the interactions of the phases.
Chemical modification	T_g, step height and the width of the transition can change; several transitions can occur.	By specific chemical modification or chemical aging such as oxidation or degradation of polymers
Fillers	The step height decreases with increasing filler content.	Hardly any effect on T_g

Thermal values of fats: DSC analysis or dropping point determination?

Dr. B. Benzler, Applikationslabor METTLER TOLEDO, Giessen

Many of the pure starting materials used in the pharmaceutical industry and in food technology can be routinely analyzed and characterized with the help of melting point determination. The situation is quite different, however, for edible oils, fats, and waxes.

Thermal values
The variable composition and different crystal modifications of such products mean that they cannot effectively be characterized by one single thermal value, e.g. the melting point.

Nevertheless, at least for comparison purposes, a number of different procedures have been developed to obtain thermal values that can be easily measured in routine analysis, e.g. softening points, dropping points, slip melting points , melting point according to Wiley and Ubbelohde, etc.

DSC
In contrast, DSC analysis, which measures the heat absorbed when the temperature of a sample is raised at a linear rate, offers many more possibilities. The result is now no longer a single temperature value, but a complete measurement curve that records all the thermal effects occurring in the temperature range investigated. This technique allows a much more detailed comparison and characterization of oils fats and waxes to be made. But can we convert the data from such complex measurement curves into the numerical values that in the end are required for comparative assessments and as characteristic values? One method often used is to measure the area between the measurement curve and the instrument baseline at discrete temperature intervals. These areas are then calculated as percentages of the total area under the melting curve and the results presented in tabular form. In the literature, the values obtained by this method are referred to as the liquid fraction, LF, or the complementary term solid fat index.

Comparison DSC - thermal values
Can the results from different methods be correlated in order to obtain a uniform set of results from various different sources? In principle, no, because in fact very different properties are measured. In the slip melting point and dropping point methods, the temperature-dependent viscosity of the sample plays an important role in addition to the actual physical melting. In comparison, DSC measures only the heat required to melt the crystallites. The following table compares the results obtained from the analysis of five different samples with both techniques. The dropping point temperatures were measured with a METTLER TOLEDO FP900 system and FP83HT measuring cell. The DSC results were obtained using a METTLER TOLEDO DSC821^e equipped with an IntraCooler accessory and shows the temperatures at which 95% of each sample (as measured by the surface area under the curve) melted.

Sample preparation and measurement
Reproducible sample preparation is essential for these measurements. With dropping point measurements, the fat was first completely melted at 65 °C and then transferred to the standard nipple using a pipette (about 0.5 ml). It was then allowed to cool at room temperature for 1 hour and then stored for 12 hours in the deep-freezer compartment of a refrigerator.

For the DSC measurements, about 10 µl of each

Fat	Dropping point in °C	T at 95% LF in °C
#1	29.2	29.3
# 2	38.1	39.8
# 3	43.7	43.9
# 4	49.6	52.1
# 5	54.7	53.5

Table: Comparison of the dropping point temperature with the temperature at which 95% has melted (DSC).
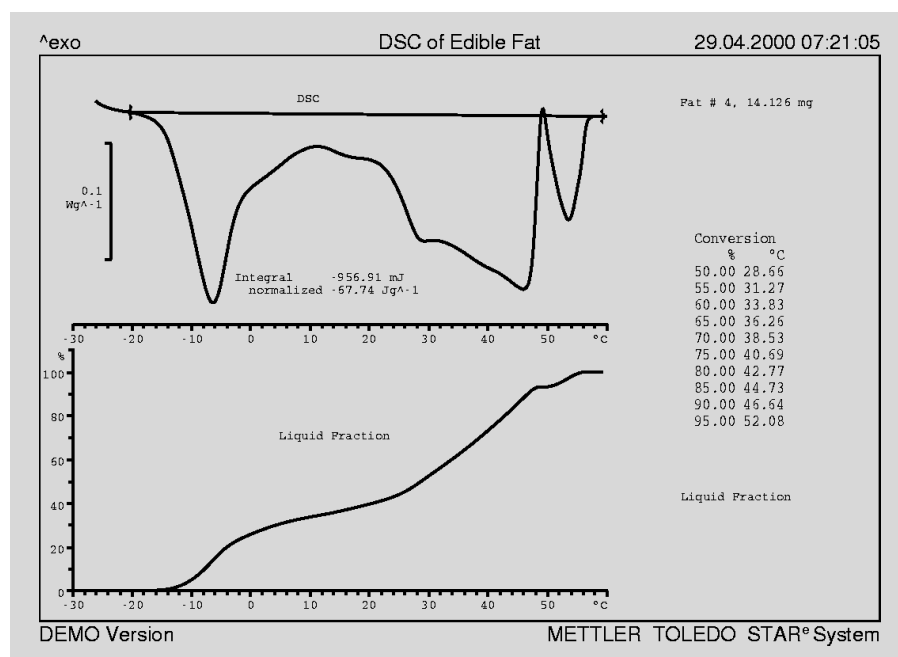

Fig. 1. The DSC curve in the upper part of the diagram shows the complex melting behavior of a sample of fat with a heat of fusion of 67.7 J/g. In the lower part of the diagram, the percentage amount of the sample that has melted at any particular temperature is shown as a curve and in tabular form between 50% and 95%.

of the liquid fat samples were pipetted into standard aluminum pans, and the sample pretreatment integrated into the DSC measurement program. This consisted of a period at 60 °C, then programmed cooling down to –30 °C at a cooling rate of 5 K/min, storage for 5 minutes at –30 °C and then the heating measurement at 5 K/min. The results of a typical measurement are shown in Figure 1. The DSC heating curve is shown in the upper part of the diagram; the area under the broad, complex melting curve was integrated in order to obtain the total heat of fusion. In the lower part of the diagram, the percentage amount of the sample that has melted at any particular temperature is shown both as a continuous curve and at discrete intervals in tabular form.

The rate at which a sample is cooled to its crystallization temperature influences the polymorphic composition of the crystallites: the more rapid the cooling, the smaller is the proportion of the stable (high melting) part. The cooling rate of 5 K/min is a good compromise between a short measurement time and degree of supercooling that is not too large.

Conclusions

The characterization of fats and oils by their dropping points has the advantage of being simple with respect to both the actual measurement and the determination of the result. The FP83HT measuring cell determines the latter automatically so that the user does not have to make any decisions at all. The only disadvantage is that this one single value can only to a limited extent describe the complex melting behavior of oils and waxes.

DSC analysis, however, yields much more information regarding the composition and the relative proportions of the fractions with respect to temperature. Although stored evaluation methods (EvalMacro) can often automatically calculate the desired numerical values from the measurement curves, a critical check and possible correction by the user is, however, often appropriate.

In both cases, the sample preparation must be clearly defined in order to obtain reproducible results. This applies in particular to the crystallization conditions for the molten fats (temperature and time).

The use of MaxRes for the investigation of partially hydrated Portland cement systems

Dr. Jordi Payá , Dr. María Victoria Borrachero and Dr. José Monzó, Grupo de Investigación en Química de los Materiales (GIQUIMA), Departamento de Ingeniería de la Construcción, Universidad Politécnica de Valencia, Camino de Vera s/n, E- 46071 Valencia (España)
 # Direktor der Forschungsgruppe GIQUIMA. E-mail: jjpaya@cst.upv.es

Introduction

In cement chemistry the following symbols are used for simplicity:
A for Al_2O_3 , **C** for CaO, **H** for H_2O, **S** for SiO_2 and **$\bar{S}$** for SO_3. For example, tricalcium aluminate, $3CaO.Al_2O_3$ becomes **C_3A** and gypsum, $CaSO_4.2H_2O$, becomes **$C\bar{S}H_2$**.

The addition of water to Portland cement initiates the setting or hardening reaction, which binds the whole mass together. The hydration of Portland cement leads to the formation of different hydrates and is a very complicated process:

- Portland cement contains various components that take up water of crystallization at different rates.
- Many different hydrates, some of which are not stoichiometric, are formed.
- The degree of crystallinity of the hydrates is low.

In the first few hours after mixing water with Portland cement, **C_3A** reacts rapidly with the formation of a number of different calcium aluminum hydrates:
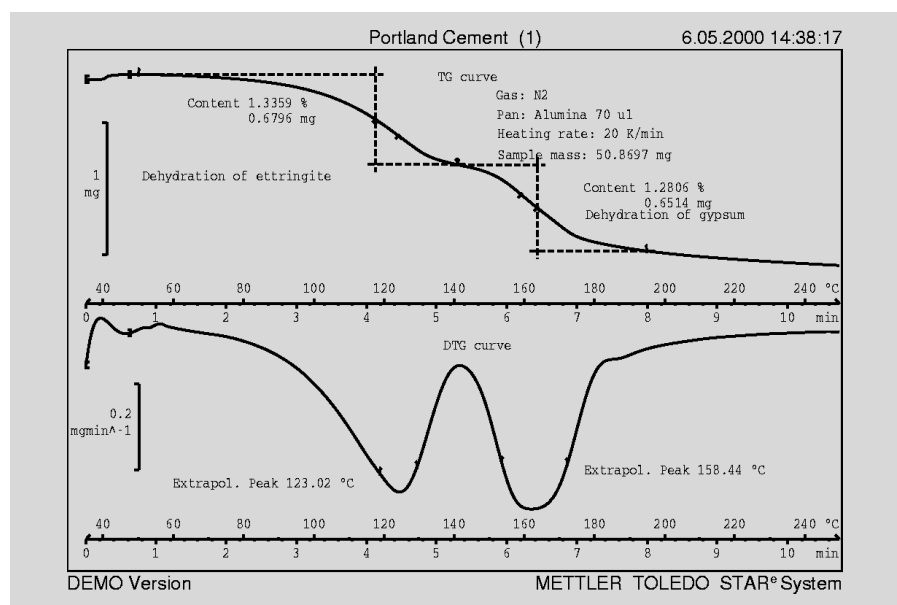
Fig. 1. TG and DTG curves of Portland cement in an open pan after 4 hours hydration.

- $3CaO.Al_2O_3.6H_2O$ (**C_3AH_6**),
- $2CaO.Al_2O_3.8H_2O$ (**C_2AH_8**) and
- $4CaO.Al_2O_3.19H_2O$ (**C_4AH_{19}**)

The presence of calcium and sulfate in the aqueous phase (dissolved gypsum) causes **C_3A** to hydrate to ettringite (**$C_6A\bar{S}_3H_{32}$**):
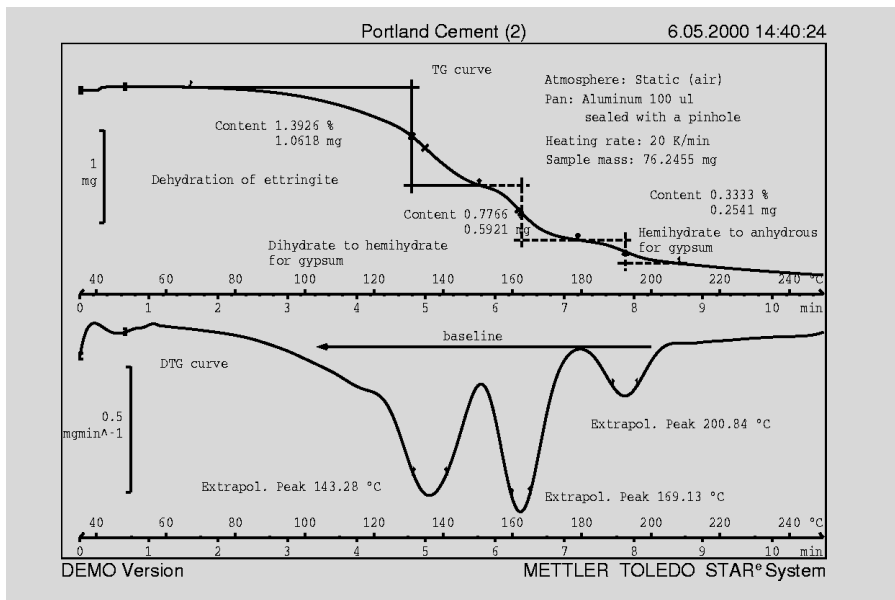
Fig. 2. TG and DTG curves of Portland cement in a self-generated atmosphere after 4 hours hydration.
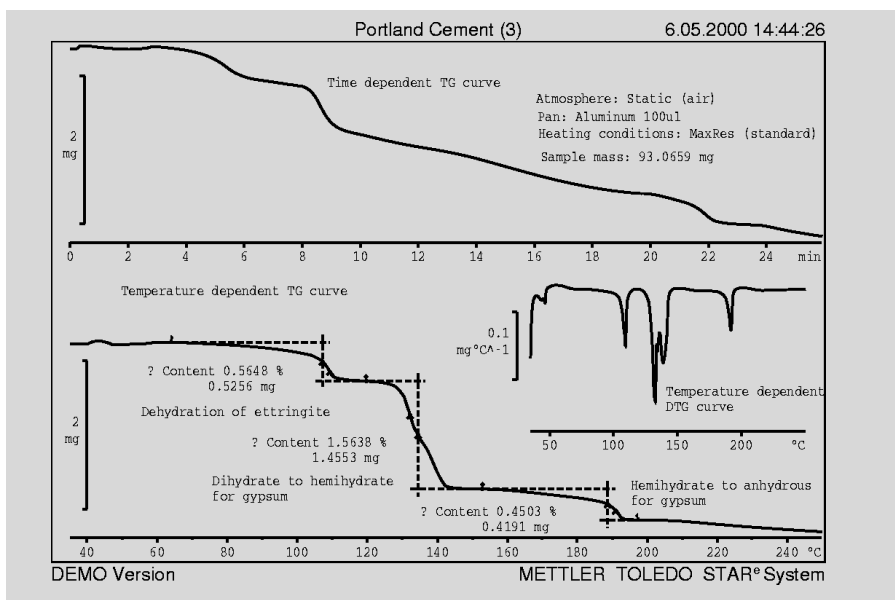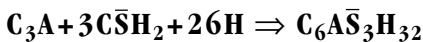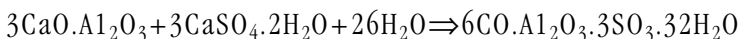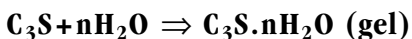

Fig. 3. MaxRes TG and DTG curves of Portland cement in a self-generated atmosphere after 4 hours hydration. Weight loss as a function of time and temperature.

$$3CaO.Al_2O_3 + 3CaSO_4.2H_2O + 26H_2O \Rightarrow 6CO.Al_2O_3.3SO_3.32H_2O$$

$$C_3A + 3C\bar{S}H_2 + 26H \Rightarrow C_6A\bar{S}_3H_{32}$$

At the same time, a small amount of colloidal calcium silicate gel (CSH) is formed from the **C₃S.**

$$C_3S + nH_2O \Rightarrow C_3S.nH_2O \text{ (gel)}$$

The interpretation of the thermogravimetric curves in the early stages of this hydration is made more difficult because the decomposition temperatures of **CSH**, ettringite and calcium sulfate dihydrate lie close together.

The thermogravimetric measurements were performed with a METTLER TOLEDO TGA/SDTA850. The adaptive event-controlled heating rate option (MaxRes [3 - 5]) was used to improve the separation of the dehydration processes.

Sample preparation

A standard mixture of Portland cement and water was allowed to set for 4 hours at 20 °C. At this stage, further uptake of water of crystallization was stopped by the addition of acetone. The solvent was then removed at room temperature under vacuum. The resulting powder was stored under nitrogen to prevent contact with moisture and carbon dioxide.

TG measurements in an open crucible

Crucible: 70 μl alumina, heating rate: 20 K/min, temperature range: 35 °C to 250 °C, purge gas: 75 ml/min nitrogen.

In an open crucible, any volatile components evolved from the sample are free to leave the crucible. Two weight loss steps can be observed (Fig. 1). The first, in the range 80 °C to 140 °C, is assigned to the dehydration of ettringite and CSH. The second, between 140 °C and 200 °C is due to the loss of water of crystallization from gypsum, which should in fact show two steps:

$$CaSO_4.2H_2O \Rightarrow CaSO_4.\frac{1}{2}H_2O + \frac{3}{2}H_2O$$

$$CaSO_4.\frac{1}{2}H_2O \Rightarrow CaSO_4 + \frac{1}{2}H_2O$$
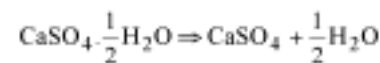
It was clearly not possible to separate the two steps in an open crucible [2].

Measurement in a self-generated atmosphere to improve the resolution

Crucible: 100 μl aluminum, with a lid with a 50 μm hole, heating rate: 20 K/min, temperature range: 35 °C to 250 °C, purge gas: stationary air atmosphere, no flow.
In a self-generated atmosphere a large proportion of the evolved products remain within the volume of the crucible. The sample is almost in equilibrium with its gas phase. The result of this is that thermal effects are shifted to higher temperature and the weight loss steps are often better separated (Fig. 2).

Under these conditions, three steps are clearly visible. The first (from 80 °C and 150 °C) is again assigned to the dehydration of **CSH** and ettringite, the second (150 °C to 180 °C) to the partial dehydration of calcium sulfate dihydrate to the hemihydrate, and the final step (from 180 °C to 210 °C) from the hemihydrate to the anhydrous form of calcium sulfate. The DTG peak of ettringite has shifted from 123 °C (in the open crucible) to 143 °C. And instead of the single peak originally observed in the open crucible at 158 °C, there are now two peaks at 169 °C and 201 °C.
From equations 4 and 5 it is clear that the ratio of the step heights for gypsum should be 3:1. In fact a ratio of 2.33:1 was obtained, which means that part of the dehydration occurred during the ettringite step.

The overlapping of the first two steps is evident from the fact that the DTG curve does not return to zero.

Measurement with the adaptive event-controlled heating rate option (MaxRes) to improve resolution

A further improvement in resolution is to be expected through the use of the MaxRes software option. The DTG signal is used to control the heating rate [3, 5] .
Crucible: 100 μl aluminium, lid with 50 μm hole, heating rate: MaxRes (standard conditions [4]), temperature range: 35 °C to 250 °C, purge gas: stationary air atmosphere, no flow.

The first step (60 °C to 115 °C) in Figure 3 is assigned to the loss of weakly-bonded water from the **CSH** gel. The weight loss between 120 °C and 150 °C is attributed to the overlapping of the dehydration of ettringite and the partial dehydration of calcium sulfate dihydrate (two peaks in the DTG curve). Finally between 150 °C and 200 °C the hemihydrate dehydrates to the anhydrous form of calcium sulfate. The ratio of the overlapped second step to the third step is now 3.47:1 and slightly greater than the 3:1 ratio expected. The difference is ascribed to the simultaneous dehydration of a certain amount of ettringite.
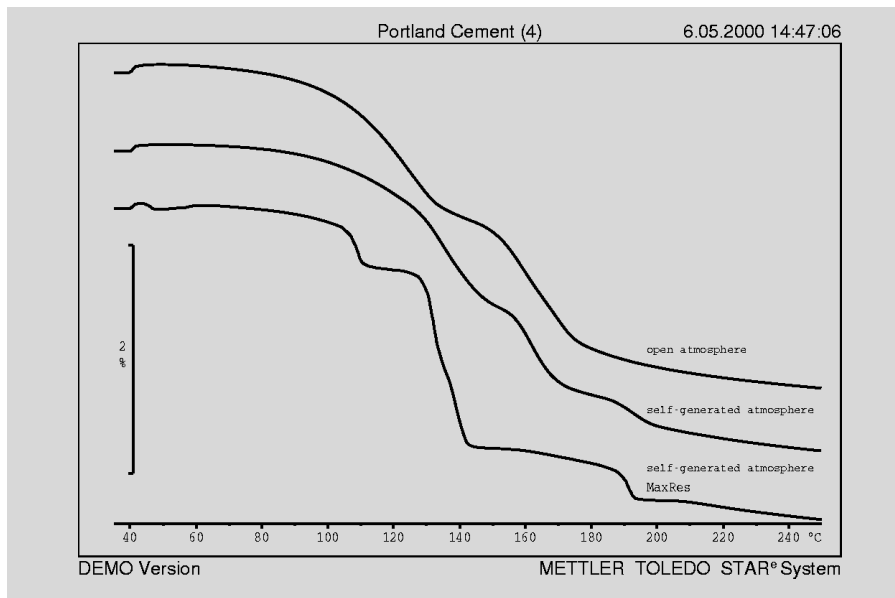

Fig. 4. Effect of the various TGA measurement techniques on the TGA curve form of Portland cement after 4 hours hydration.

Figure 4 summarizes the improvement in the resolution of the TGA curves in one diagram. Thanks to the use of MaxRes, the formation of ettringite in cement/water mixtures can be quantitatively measured by subtracting the height of the hemihydrate dehydration step multiplied by three from the weight loss in the range 120 °C to 150 °C (the second step).

Literature

[1] P.C. Hewlett (Ed). Lea´s Chemistry of Cement and Concrete, 4th edition, Arnold, London, pp. 241-298 (1998)

[2] F. Gomá . El Cemento Portland y otros Aglomerantes. Editores Técnicos Asociados SA, Barcelona, pp. 27-31 (1979).

[3] USER COM 4. Information for user of METTLER TOLEDO thermal analysis systems. December 1996, page 4.

[4] B. Schenker and R. Riesen. MaxRes: event-controlled adaption of the heating rate. USER COM 6, December 1997, pp. 10-12.

[5] R. Riesen, Adjustment of heating rate for maximum resolution in TG and TMA (MaxRes), J. Thermal Anal. 53 (1998) 365 – 374.

Vitrification and devitrification phenomena in the dynamic curing of an epoxy resin with ADSC

S. Montserrat, Y. Calventus und P. Colomer, Departament de Màquines i Motors Tèrmics, Universitat Politècnica de Catalunya, Carrer de Colom 11, E-08222-Terrassa, España

Introduction

Alternating differential scanning calorimetry (ADSC) is a DSC technique in which a periodically varying temperature is superimposed on a linear heating rate. In the case of a sinusoidal modulation of amplitude A_T and frequency ω, the heating rate, β, is described by the equation:

$$\beta = \beta o + AT \cos (\omega t) \qquad (1)$$

In conventional DSC, the temperature program is defined by the initial and final temperatures and the heating rate. In ADCS, however, in addition to the underlying heating rate βo, there are two additional parameters, namely the modulation amplitude A_T and the modulation frequency ω. These parameters must be carefully chosen in order to obtain meaningful information from the experiment (see also the article in USER COM 6).
The modulation of the heating rate results in a modulated heat flow signal, Φ. This modulated signal is subjected to Fourier analysis and separated into different components. One of these components is the total heat flow, which corresponds closely to the signal obtained from a conventional DSC measurement at a heating rate of βo. In addition, the curve of the complex heat capacity $|C_p*|$ is calculated according to the equation:

$$\left| C_p^* \right| = \frac{A_\Phi}{A_\beta} \qquad (2)$$

where $A\Phi$ and $A\beta$ are the amplitudes of the heat flow and the heating rate respectively. The phase angle between the modulated heating rate and the modulated heat flow is also calculated. This allows certain assertions to be made about relaxation processes in the sample.
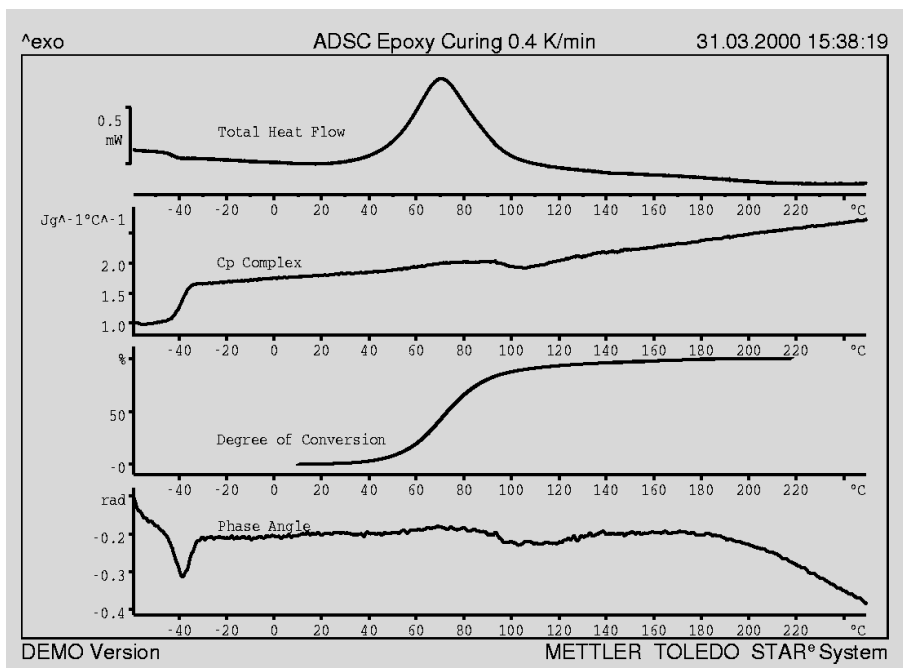
Fig.1. Total heat flow, complex heat capacity and phase angle of an amine-hardened epoxy system (average heating rate 0.4 K/min, amplitude 0.2 K, period 1 min). The degree of curing is shown above the DSC curve.
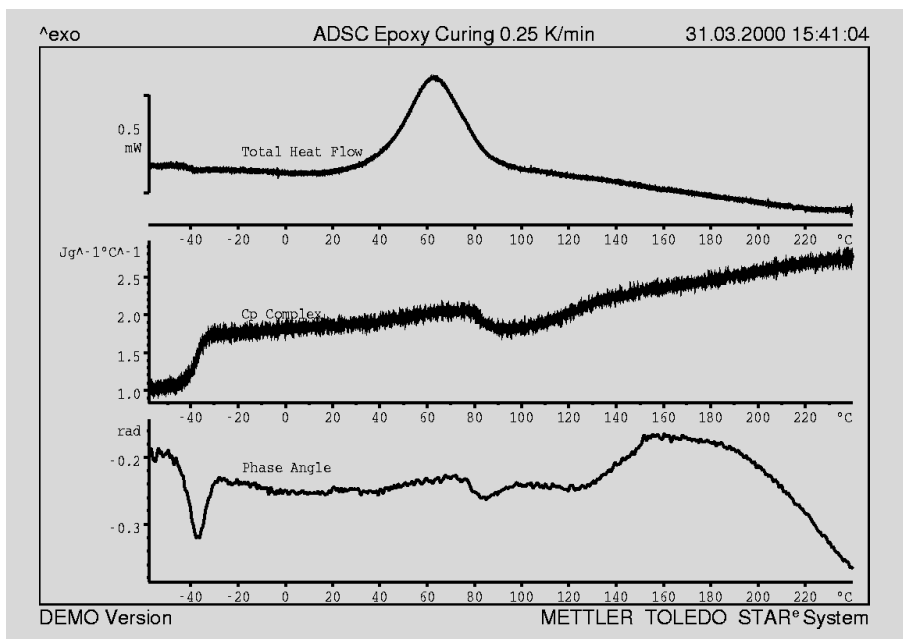

Fig.2. The same as in Figure 1 but measured with an average heating rate of 0.25 K/min.

The use of ADSC allows the isothermal curing of epoxy resins to be investigated. Of particular interest in this respect are vitrification and the determination of the temperature-time-transformation diagram [2, 3].
This article describes how the ADSC technique can be used to investigate dynamic curing. Vitrification (liquid→solid transition) followed by devitrification (solid→liquid transition) can be observed on the heat capacity and the phase angle curves if the heating rate is sufficiently slow. The corresponding temperatures are determined from the |Cp*| signal and en-

tered in the continuous heating cure diagram (CHT diagram). The CHT diagram shows the temperatures and times that are required to reach these transitions at various different constant heating rates (4). Analogous to the isothermal TTT diagram, the CHT diagram is used to investigate the properties and the influence of curing conditions on such resins.

Experimental details
The epoxy system investigated was an epoxy resin based on a diglycidyl ether of bisphenol A (DGEBA) (Araldite LY564) and cured

with an amine hardener based on 3,3'-dimethyl-4,4'-diaminodicyclohexylmethane (HY 2954). The fully cured resin exhibited a maximum glass transition temperature , Tg_∞, of 159 °C measured by ADSC.

The measurements were performed using a METTLER TOLEDO DSC821^e equipped with an IntraCooler cooling accessory. The results were evaluated with the S**TA**R^e software.
An amplitude of 0.2 K and a period of 1 minute were used for all the measurements described in this article. The average heating rate was varied between 1 and 0.1 Kmin^{-1}. All necessary blank and calibration measurements were performed before the actual measurements in order to ensure optimum results.
The experiments were performed with sample weights of about 10 mg in standard Al pans.

Results and discussion
Figure 1 shows the total heat flow, the complex heat capacity and the phase angle of an epoxy amine hardener system during dynamic curing (average heating rate 0.4 K/min, amplitude 0.2 K, period 1 min). The glass transition of the uncured resin is visible in all three signals (endothermic shift of the DSC curve, the increase in the c_p curve and the relaxation peak in the phase angle signal). Evaluation of the DSC curve gave a value of −42 °C (midpoint) for the glass transition temperature, Tg_0.

At an average heating rate of 0.4 K/min, the exothermic curing reaction begins at about 20 °C. The maximum reaction rate occurs at about 70 °C and curing is completed between 180 °C and 200 °C. The integration of the peak using a linear baseline yields a value of 460 J/g for the heat of cure. As with conventional DSC, the conversion of the reaction can be determined by dividing the partial areas by the heat of fusion (Fig. 1). During the course of the reaction, the heat capacity increases due to the crosslinking. The constant phase signal shows that no relaxation processes occur.

The heat capacity decreases at about 90 °C and then increases again at about 110 °C. These changes of c_p correspond to the vitrification (at 80% to 90% conversion) and
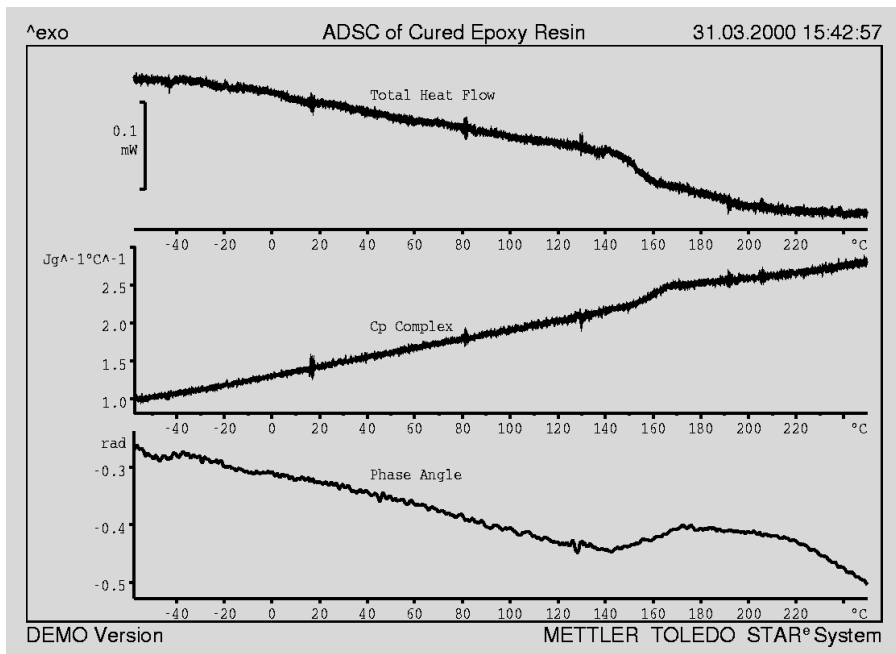
Fig. 3. Total heat flow, complex heat capacity and phase angle of a fully cured epoxy amine hardener system (average heating rate 0.4 K/min, amplitude 0.2 K, period 1 min). This is the second measurement of the same sample from Figure 1.
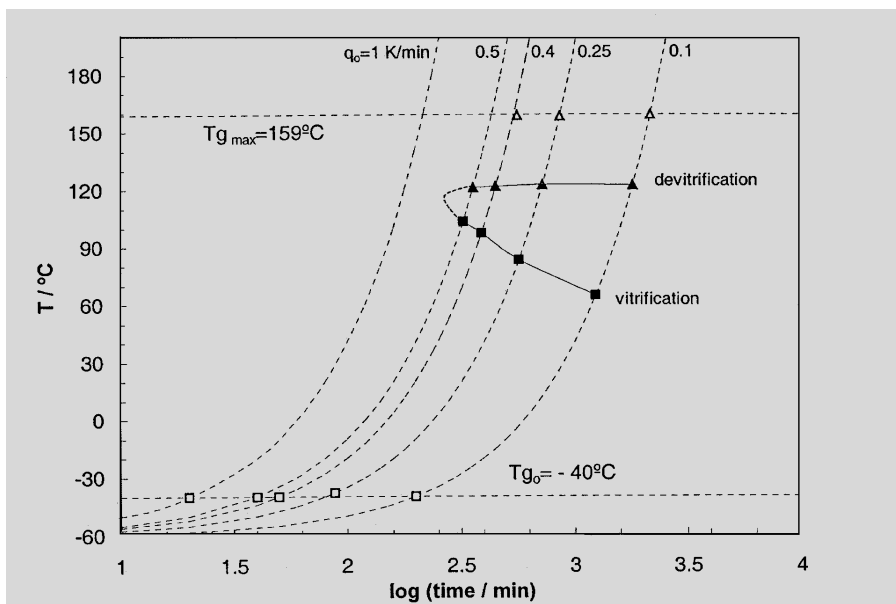

Fig. 4. Continuous heating transformation cure diagram (CHT diagram) of the measured epoxy resin amine hardener system. The dashed lines show the average heating rates used. Filled black squares mark the vitrification temperatures, and black triangles the devitrification temperatures. White triangles show the glass transition temperatures of the fully cured resin, and white squares the glass transition temperatures of the uncured resin-hardener mixture.

then the subsequent devitrification (at 95% conversion) of the epoxy resin. The epoxy resin used shows the vitrification more clearly than the devitrification. Values of 97 °C and 121 °C were determined for the midpoints of the two effects.

At lower heating rates, vitrification occurs at a lower temperatures, while devitrification is shifted to slightly higher temperatures (Fig. 2). This means that the separation of the two effects increases with decreasing heating rate. This has also been

observed with other amine-hardened and anhydride-hardened systems using torsional braid analysis [4]) and temperature modulated DSC [5].

A second ADSC measurement of the fully cured resin gave a value for the maximum glass transition temperature of the system, Tg_∞, of 159 °C (midpoint of the |Cp*| signal) and a c_p change of about 0.20 $Jg^{-1}K^{-1}$ (Fig. 3). This value for the c_p change is smaller than that at Tg_0 (0.6 $Jg^{-1}K^{-1}$) and is in agreement with conventional DSC mea-

surements made on other epoxy systems [6]. As expected, the glass transition can be observed in the DSC curve and as a relaxation peak in the phase angle.

The different vitrification and devitrification temperatures measured with various heating rates are shown in the CHT diagram (Fig. 4). They define the region within which the glass transition occurs. The values of Tg_0 (-40 °C) and Tg_∞ (159 °C) are also shown. In other epoxy resin systems, devitrification does not occur until Tg_∞ [4, 5]. According to Verchère et al [7], the reason why devitrification occurs at a lower temperature in our system is the effect of steric hindrance of the methyl group, which inhibits the reaction with the amine hydrogen atom. Consequently, the fully cured epoxy is only obtained on further heating up to 250 °C.

Conclusions

The non-isothermal ADSC technique allows the measurement of vitrification and devitrification temperatures during the curing of epoxy resin systems. This is not possible with conventional DSC. The data obtained can be used to construct a CHT diagram. Compared with torsional braid analysis, ADSC has the advantage of determining the degree of cure at the same time.

Literature

[1] C. T. Imrie, Z. Jiang, J. M. Hutchinson, *Phase correction in ADSC measurements in glass transition, USER COM No.6, December 97, p.20-21*

[2] S. Montserrat, *Vitrification in the isothermal curing of epoxy resins by ADSC, USER COM No.8, December 98, p.11-12*

[3] S. Montserrat, I. Cima, *Thermochim. Acta, 330 (1999) 189*

[4] G. Wisanrakkit, J. K. Gillham, *J. Appl. Polym. Sci., 42 (1991) 2453*

[5] G. Van Assche, A. Van Hemelrijck, H. Rahier, B. Van Mele, *Thermochim. @Ïfa, 286 (1996) 209*

[6] S. Montserrat, *Polymer Commun., 36 (1995) 435*

[7] D. Verchère, H. Sautereau, J. P. Pascault, C. C. Riccardi, S. M. Moschiar, R. J. J. Williams, *Macromolecules, 23 (1990) 725*

Expansion and shrinkage of fibers

Introduction

Fibers are produced worldwide in enormous quantities. More than 20 million tons of synthetic fibers and 20 million tons of natural fibers are manufactured each year. The total length of these fibers corresponds to about 10 000 times the distance from the earth to the sun.

A characteristic feature of a fiber is that its length is much greater than its diameter. The great anisotropy of the microstructure and the physical properties originating from spinning and stretching processes are two of the main reasons for the special properties and peculiarities of fibers [1, 2]. Spinning, stretching and annealing are in fact the most important steps in the manufacture of fibers. These processes determine properties such as the modulus of elasticity (Young's modulus, E) and toughness that are required for the application envisaged. Coloring properties, shrinkage (contraction of fibers) and thermal stability are determined by the size, number and orientation of the crystallites, as well as the molecular structure in the amorphous regions. Thermomechanical analysis (TMA) in particular, as well as DMA, DSC, TGA and TOA are all excellent techniques for the investigation of the effects of temperature and mechanical loading on fibers and yarns. They allow the relationship between structure, properties and the manufacturing process [3] to be investigated. Very often comparative measurements under identical conditions are sufficient to characterize transition temperatures, expansion and shrinking behavior. TMA measurements also yield numerical values such as the coefficient of linear expansion, Young's modulus, E, and the force of contraction as a function of temperature.

Terminology

Fiber strength is normally characterized by its linear density. The SI unit is the tex. The unit decitex (dtex) is often used, which is the weight in grams of a length of 10 000 m of fiber (or in other words: 1 dtex = 1 μg/cm). In order to compare fibers of different linear density with respect to their expansion behavior, the samples are usually heated under the same tensile force, e.g. 0.1 mN/dtex.

Example: a piece of silk thread has a length of 22 cm and a weight of 0.363 mg. The linear density is therefore 16.5 dtex. The thread was subjected to a load of 0.002 N in the TMA.

The average linear coefficient of expansion, α_l, in the temperature range T_1 to T_2 can be calculated from the change in length in this temperature range, ΔL, and the original length L_0 according to the equation:

$$\alpha_1 = \frac{\Delta L}{L_0 (T_2 - T_1)}$$

The module of elasticity, E, is determined by the ratio of the tensile force to the expansion:

$$E = \frac{\Delta F / A}{\Delta L / L_0}$$

Here ΔF is the change in the tensile force, A is the cross-sectional area of the fiber and DL is the change in length as a result of the change in the tensile force. This assumes that the change in length, DL, is small compared with the total length, L_0.

In the TMA, the change in the tensile force is caused by a stepwise change in the load. During the heating measurement, the tensile force exerted on the sample is, for example, modulated with a constant value of 0.06 N with a period of 12 s and an amplitude of 0.01 N. This mode of operation is known as Dynamic Load TMA (DLTMA).

Experimental details

The measurements described in this article were performed with a METTLER TOLEDO STARe System and the TMA/SDTA840 module. The samples were prepared for measurement by mounting them in the fiber attachment accessory. The fibers were placed in copper clips and fixed in place by mechanically squeezing the clips together. The effective length of fiber between the two clips was always 13 mm. Samples prepared in this way were mounted between the hooks of the sample holder (see Fig. 1). During the heating measurement, the soft-

Sample	Description	Linear density [dtex]	Tensile force in the TMA [N]
Wool	Woll yarn	1157	0.116
Cotton	Cotton yarn, merceried	298	0.030
Silk	Silk thread	17	0.002
Hemp	Hemp fibers from a piece of string	57	0.006
Hair (horse tail)	Horse hair, black from a horse tail	324	0.033
Hair (human)	Human hair	47	0.005
PAN	Polyacrylnitril, yarn	219	0.022
PA 66 bulky	Nylon, crimped (Helanca)	252	0.025
PA 66	Nylon yarn	1400	0.144
PA 66	Nylon, 6 fibers (from yarn)	44	0.004
PA 66	1 fiber, 0.1 mm (Viscosuisse type 162)	90	various forces
PET	1 fiber 0.048 mm (Viscosuisse, type 200)	25	0.003
PET	1 fiber, 0.1 mm (Viscosuisse, type 260)	108	0.011
PE	1 fiber (Dyneema®)	13	0.002
Kevlar	Several fibers	85	0.009
Carbon	Several fibers	101	0.050
Aluminum	Aluminum wire, 0.3 mm	-	0.050
Copper	Copper wire, 0.2 mm	-	0.050
Fused Silica	Quartz fiber glass 0.1 mm	-	0.050

Table 1. List of the various fibers measured with details of their origin, linear density and the tensile force used in the experiment.

ware compensates for both the expansion of the clips (the effective length is 1 mm) and the expansion of the quartz sample holder.

The sample temperature was checked and adjusted using an indium melting point reference sample. To do this, two small pieces of indium with a total weight about 10 mg were squeezed together around a sample of fiber (see Fig. 1). This allowed the melting point of indium to be measured several times at different heating rates - the melting point of the fiber must of course be appreciably higher. The thermocouple for the measurement of the sample temperature was positioned about 3 mm away from the center of the fiber. As can be seen in Figure 2, the SDTA signal records the melting of the indium sample. The SDTA signal is the temperature difference between the measured temperature of the sample and the program temperature [4]. The SDTA curve in Figure 2 shows a small peak due to the melting of the in-

Fig. 2. TMA and SDTA curves showing the temperature check with indium on a PET fiber (see Fig.1). Heating rate: 10 K/min, stationary air atmosphere. SDTA curve: exothermic in the upward direction; TMA: expansion in the upward direction.
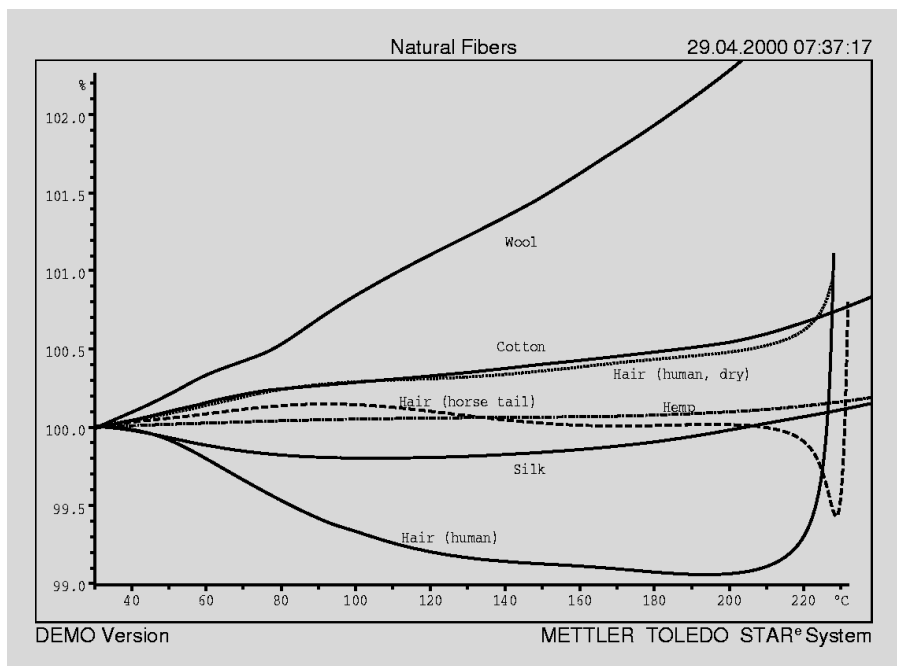
Fig. 3. Natural fibers (see Table 1). For clarity, dry hair is shown as a dotted curve and horsehair as a dashed curve.

Fig. 1. Quartz glass sample holder with fiber sample mounted. A piece of indium is attached to the fiber.

dium standard. The onset temperature was evaluated in the same way as for DSC curves. The TMA curve also shows a small step in the same temperature range. The reason for this is that the temperature of

the short section of fiber that is enclosed by the indium sample remains constant. This section of the fiber does not therefore expand while the indium melts.

The fiber samples were measured in the range 30 °C to 270 °C at a heating rate of 10 K/min in a stationary air atmosphere with a tensile force 0.1 mN/dtex. Table 1 shows a list of the fibers used for the measurements. Any deviations from the experimental conditions given above are noted together with the results of that particular sample.

Results
Shrinking behavior
Examples of TMA curves of natural fibers, synthetic fibers, and special fibers and wires are shown in three separate diagrams. A detailed discussion of the thermoanalytical measurement of fibers is given in reference [2].

Natural fibers (Fig. 3)
Human hair and silk both shrink (i.e. contract) initially due to drying. Decomposition begins above 220 °C and the fibers rapidly tear. Horsehair and hemp show

relatively little change in length below 200 °C (< 0.1 %) under the tensile force used. Wool, however, expands in the same range by more that 2 %. Dry human hair shows a similar behavior. Cellulose fibers (e.g. cotton and hemp) show far greater thermal stability compared with fibers of human or animal origin and expand until they decompose and break at about 400 °C.

Synthetic fibers (Fig. 4)

Synthetic fibers, in contrast to fibers of natural origin, nearly always show a marked shrinkage that is very dependent on the manufacturing process, and also behave thermoplastically. With special ex-

identical in form to those of an individual fiber taken from the same yarn. This comparison shows the excellent reproducibility of such measurements (see PA66 with 44 and 1400 dtex). The PET fibers used have different type designations and their curve forms also show somewhat larger differences. A comparison of the curve of PA66 (252 dtex) to the other PA66 curves shows how great the influence of processing on thermal expansion can be. Polyacrylonitrile, (PAN), is dimensionally very stable up to about 130 °C and shows only small changes in length of less than 0.5%. At higher temperatures, however, PAN expands more rapidly than wool for example.

α_l for aluminum and copper are entered in the diagram (calculated from the average slope over a range of 40 K). The literature values for the relevant temperature ranges are also given (upper left).

Effect of conditioning

TMA is not just a technique that can be used to measure a new sample of a fiber. It can also be used to condition samples thermally. Both the temperature and the applied tensile force have a large effect on the subsequent thermal behavior, which again can then be measured with TMA. This conditioning procedure allows process conditions to be simulated or understood, and their effect on the thermal behavior of the fibers to be investigated. To illustrate this, a polyamide fiber was cooled with different tensile forces and then heated again using a weak tensile force of 0.1 N (see Fig. 6a). Figure 6b shows the heating curves for different values of the tensile force, whereby the cooling beforehand was performed with a tensile force of 0.1 N. The larger the tensile force used on cooling, the greater was the shrinkage afterward on heating. If the tensile force used for cooling was lower that used for the subsequent heating, then the fiber expands until the force of contraction is sufficiently large to counteract the expansion.

Determination of the force of contraction

One would sometimes like to determine the force of contraction that develops when a fiber is heated but held at constant length. This type of measurement is only possible if the TMA is equipped with a suitable accessory (e.g. a converter). If, however, the heating curves of individual samples of the same fiber are measured with different tensile forces in the TMA, then the force of contraction can be determined directly as a function of temperature from the measurement curves (Fig. 7). The temperatures at which the length of the fiber after thermal expansion is the same as its initial length are read off from the array of curves. In Figure 8, the temperatures corresponding to the points of intersection of each TMA curve with the horizontal straight line through the starting point (at 30 °C) are plotted as a function of the force applied. The data points show a pronounced increase of the force of contraction above the glass transi-
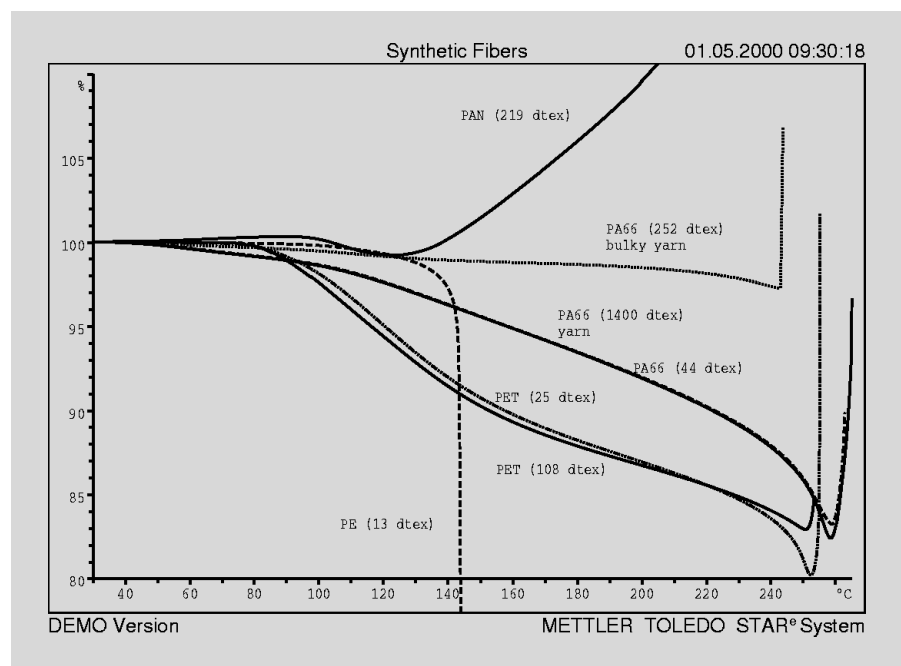
Fig.4: Synthetic fibers made from different polymers (see Table 1)

tremely orientated fibers (e.g. Kevlar, Fig. 5), the degree of shrinking is low (< 0.5%) up to high temperatures (450 °C) and is also reversible from the second heating measurement onward. Normal, irreversible shrinkage begins above the glass transition temperature (e.g. PET: 80 °C; PA66: <50 °C depending on the moisture content; PAN: 90 °C) and increases shortly before melting. Melting is indicated by a very rapid increase in length of the fibers. The extremely rapid shrinkage of PE before melting is a result of the special manufacturing process, in which the fibers are stretched after the spinning process. Since the measurement force is normalized to a linear density (0.1 mN/dtex), the TMA curves of a yarn (with many fibers) are

Special fibers and metal wires (Fig. 5)

Carbon fibers and quartz glass fibers show only a very low degree of expansion over a wide range of temperature. Quartz glass fibers are brittle and are therefore difficult to mount. They are, however, useful as "inert" material for the determination of the baseline (blank curve).

The fiber attachment can also be used to mount thin wires. The example shows the determination of the linear coefficient of expansion (α_l) of aluminum and copper wires. In contrast to polymer fibers, α_l for metals is only slightly temperature dependent and the values are much smaller (e.g. 25 ppm/K for aluminum compared to 125 ppm/K for wool). The mean values of
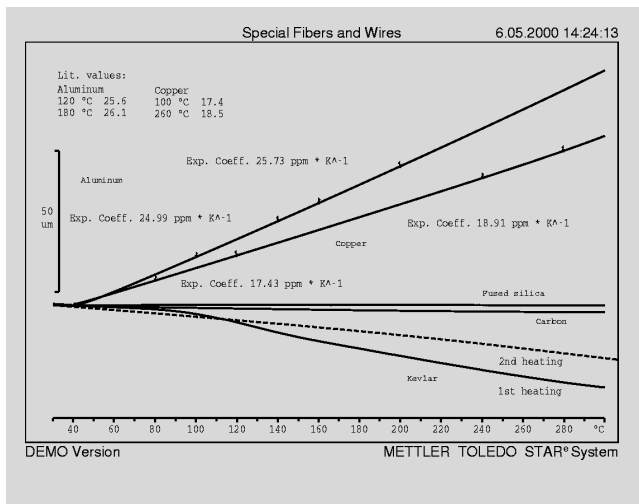
Fig. 5. Special fibers and metal wires

tion temperature of 80 °C. Recrystallization and relaxation processes [5] that take place above 100 °C are the cause of the slow decrease of the force of contraction at higher temperatures.

The great advantage of TMA measurements with different loads is that with relatively few measurements, the force of contraction and the shrinking behavior can be simultaneously measured without having to change the configuration of the instrument. A second heating measurement performed using the same measurement parameters does not show any force of contraction.
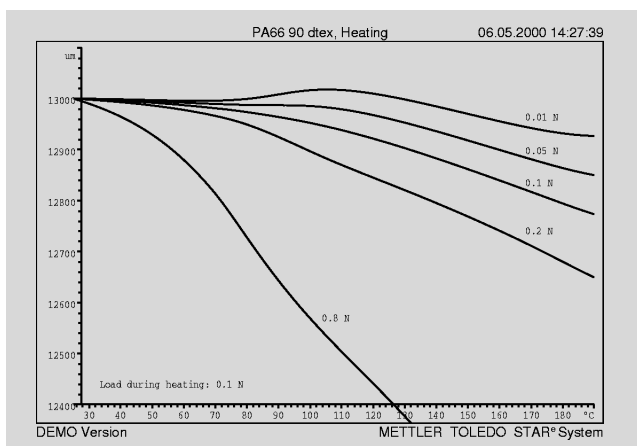
Fig. 6a. Thermal conditioning and measurement of the expansion/shrinking behavior of a Nylon fiber (PA66, 90 dtex) using different tensile forces. The fibers were conditioned by cooling from 190 °C to 35 °C under a tensile force of 0.1 N. The subsequent measurements were performed with the tensile forces noted next to the curves.
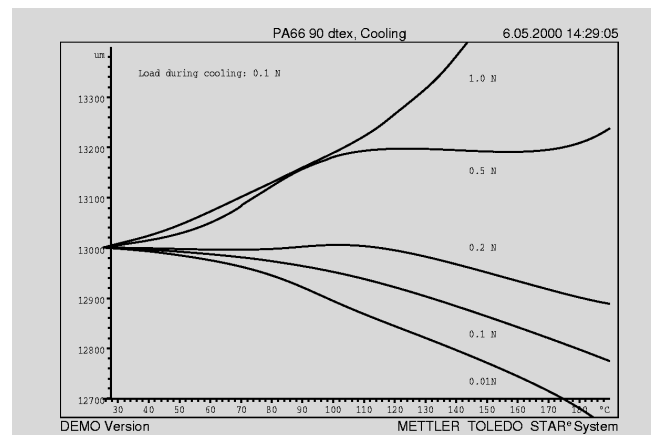
Fig. 6b. Measurement of the expansion and shrinking behavior of a Nylon fiber (PA66, 90 dtex) after conditioning the fiber by cooling from 190 °C to 35 °C under the tensile forces noted next to the curves. The subsequent measurements were performed with a tensile force of 0.1 N.
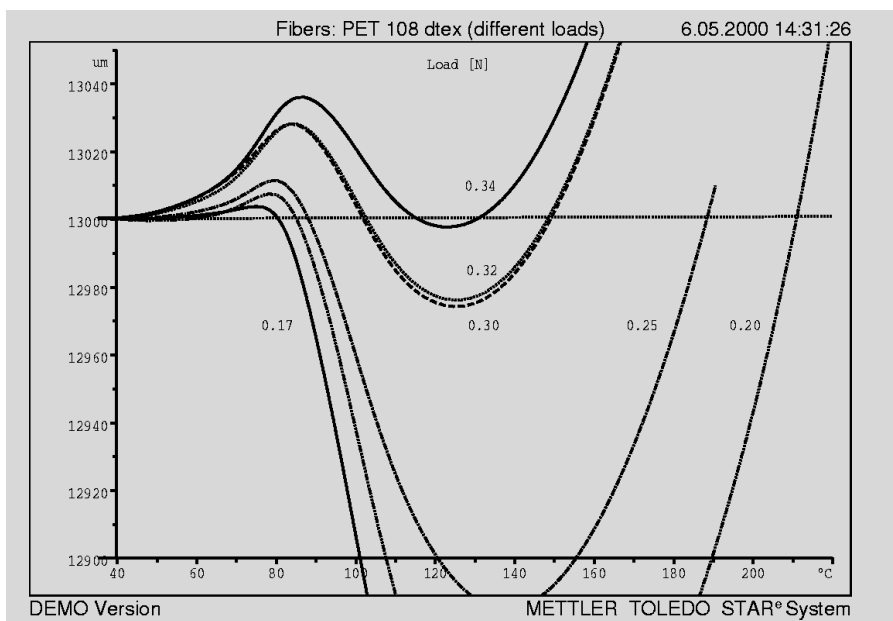
Fig. 7. TMA curves of PET fibers (108 dtex). A different constant tensile force was used for each sample for each heating run (30 °C to 220 °C at 10 K/min). This yields an array of shrinkage/expansion data curves.

Determination of Young's modulus

In addition to the investigation of shrinkage, one of the main applications of thermomechanical analysis for the characterization of fibers is the determination of Young's modulus, E, and its dependence on temperature. With the TMA/SDTA840, a periodically changing force is used instead of the constant force (DLTMA operating mode). The resulting expansion is used in the evaluation to calculate the value of Young's modulus. During heating, the sample is modulated with a periodic, step-wise change of force (period usually 12 s, amplitude typically 0.01 N). This also allows the temperature dependence of Young's modulus to be measured during shrinking. Figure 9 shows the DLTMA curves of a PET fiber. Young's modulus is calculated from the amplitude of the peri-
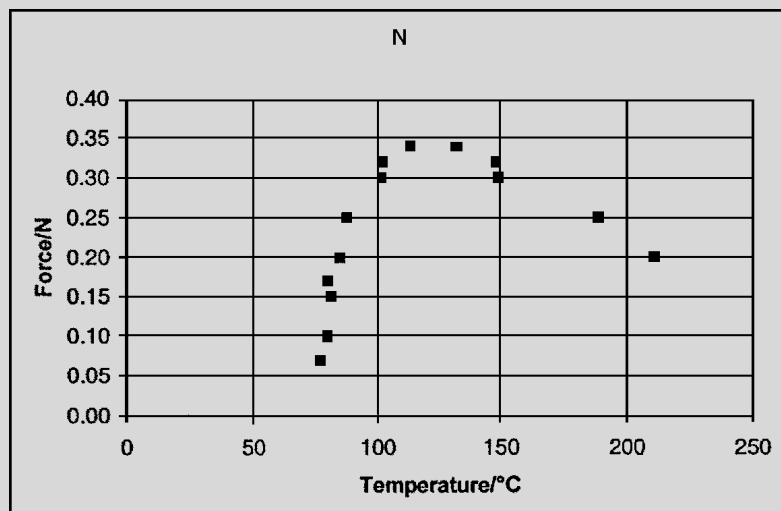
Fig. 8. The force of contraction of PET (108 dtex): the data points were determined from the curves in Figure 7 as described in the text.

Fig. 9: DLTMA curves of a PET fiber (108 dtex) showing the first and second heating runs: heating to 220 °C at 10 K/min with a tensile force which changes every

odic change of length (storage modulus) using Fourier analysis (see lower diagram in Figure 9). The value of Young's modulus starts to decrease as soon as the glass transition begins (onset 68 °C). It in fact decreases by a factor of ten due to the glass transition. A comparison of the first and second heating curves shows that at low temperatures the value of the Young's modulus for the stretched fiber is somewhat larger than that of fiber after it has undergone shrinkage. Above 120 °C, i.e. above the glass transition, the values of Young's modulus are the same because the physical conditions are similar.

Conclusions

The TMA measurement technique and the evaluation the resulting curves is an excellent way to characterize the expansion and shrinking behavior of fibers. Effects originating in the manufacturing process and subsequent processing steps can be detected and described. The TMA curves allow properties such as the glass transition temperature, the degree of shrinking and the melting temperature to be determined. Values of the expansion coefficients, Young's modulus and the force of contraction can be calculated and displayed as a function of temperature. The copper clips allow very fine

fibers and even thicker yarns and wires to be reproducibly mounted - this is of course absolutely essential for accurate results. The measuring system can also be used to condition fibers at different temperatures, or under different tensile forces or gas atmospheres. DMA, DSC, TGA and thermo-optical analysis are additional techniques that can be used to determine the properties of fibers.

Literature

[1] L.H. Sperling, Introduction to physical polymer science, 2nd ed., Wiley-Interscience, New York (1992), p. 263.

[2] M. Jaffe, J. D. Menczel, W. E. Bessey, Chapter 7 in Thermal Characterization of Polymeric Materials, 2nd ed. (E. A. Turi, Ed.), Academic Press, New York (1997) 1767 - 1954.

[3] ibid., Seite 1785.

[4] J.A. Foreman, R. Riesen, G. Widmann, Thermal Trends, Vol. 5, No. 3 (Summer 1998), 18.

[5] R. Riesen, J.E.K. Schawe, J Thermal Analysis, Vol. 59 (2000) 337-358.

The cooling performance of the DSC821e

Introduction

In many DSC experiments the sample has to be cooled under full control at a constant cooling rate, i.e. program cooled. Toward the end of such a measurement, red brackets may appear on the measurement curve, indicating that the cooling capacity is no longer able to maintain the given cooling program. This of course depends on the type of cooling option used and the cooling rate chosen. In order to complete a cooling program without these warning signs appearing, one needs to know the lowest temperature which can be reached at a given cooling rate. This article presents measured cooling curves which can be used to estimate the maximum cooling rate as a function of the end temperature.

Fig. 1. Cooling curves for the DSC821e with air cooling, IntraCooler and liquid nitrogen cooling.

Fig. 2. Cooling rates for different DSC821e cooling options (air cooling, IntraCooler, liquid nitrogen).

Free cooling of the DSC821e

To measure the maximum cooling rate, a temperature program consisting of two isothermal segments (start temperatur and end temperature) is used. When the segment changes, the measuring cell tries to reach the temperature of the second segment as rapidly as possible. The rate of temperature change then corresponds to the maximum possible cooling rate at that paricular temperature. Figure 1 shows the cooling curves measured in this way for various cooling options.

On the assumption that cooling is above all the result of thermal conduction, the cooling behavior can be described by a simple exponential equation. In this case, the cooling rate τ at a particular temperature, T, can be estimated from to the equation

$$\beta = \frac{1}{\tau} \cdot \left(T_0 - T\right) \qquad (1)$$

where τ is the time constant characteristic for the DSC furnace and T_0 is the temperature of the cooling flange. The value of T_0 is about -70 °C for the IntraCooler and about 22 °C for air cooling. This model assumes that the temperature of the cooling flange is constant and that the time constant of the instrument can be described by a single value. To a good approximation, this is in fact the case for normal air cooling, the IntraCooler or normal cryostats. The cooling time constant is about 4 minutes. If the system is cooled with liquid nitrogen, the temperature of the cooling flange no longer remains constant and the cooling behavior can no longer be described by the above equation.

Figure 2 shows the cooling rates as a function of temperature for the various cooling options available. To a good approximation, the results for air cooling and cooling with an IntraCooler are given by the straight lines described by equation 1, where the slope corresponds to the recipro-
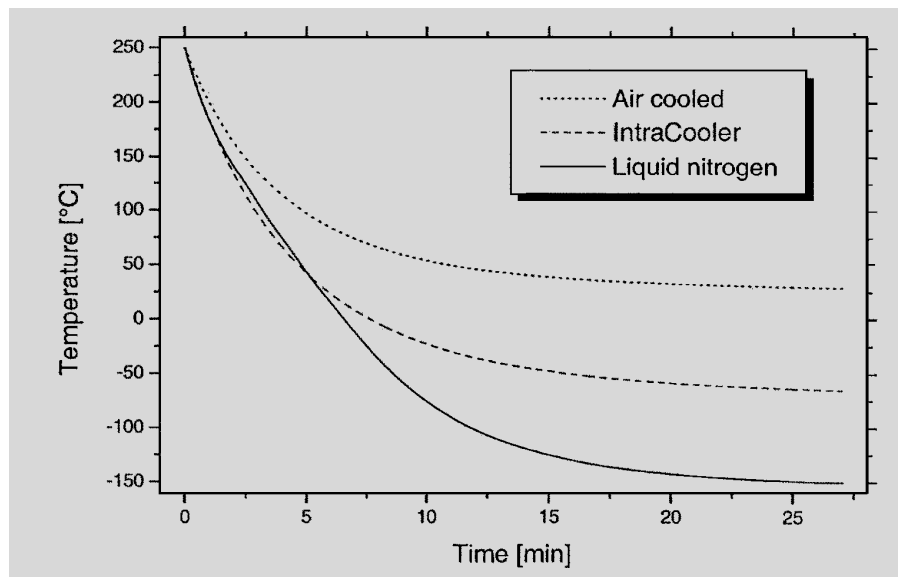
Temperature [°C]	Cooling range with different cooling options [K/min]		
	Air cooled	IntraCooler	Liquid nitrogen
-40	-	4	27
-20	-	8	30
0	-	12	31
20	-	16	30
40	2	20	32
60	6	25	35
80	11	19	34
100	15	34	34

Table 1. Maximum cooling rates for different DSC821e cooling options at various temperatures.

cal of the cooling time constant. With liquid nitrogen cooling, three different "cooling ranges" can be distinguished, which are determined by the mode of operation of the feedback control circuit that regulates the amount of liquid nitrogen supplied. Above about 100 °C, only a small amount of liquid nitrogen is used for cooling and the cooling flange remains at an almost constant temperature. Between 100 °C and about -100 °C more and more liquid nitrogen is supplied, the cooling power increases and the cooling rate has a value that is more or less independent of the actual furnace temperature. Below -100 °C, the cooling flange reaches its lowest value (typically about -170 °C), and the cooling rate decreases rapidly. The diagram shows that liquid nitrogen cooling is superior to IntraCooler cooling except in the range between about 100 °C and 150 °C. Table 2 summarizes the maximum cooling rates for the 3 cooling options.

One would often like to know how long the measuring cell takes to cool down from the starting temperature, T_1, to the final temperature, T_2. For cooling options whose cooling behavior can be described by the time constant, τ, the time can be estimated with the help of equation (2).

$$t_{T_1 \to T_2} = \tau \cdot \left[\ln(T_1 - T_0) - \ln(T_2 - T_0) \right] \quad (2)$$

T_0 is the temperature of the cooling flange. The value of T_0 is about -70 °C for the IntraCooler and about 22 °C for air cooling. With liquid nitrogen cooling, the cooling behavior can no longer be described with a time constant, so that equation (2) can no longer be used. The cooling time constant τ is about 4 minutes. This is valid for the IntraCooler, air cooling and cryostat cooling).

Conclusions

The most rapid cooling rates can be achieved using liquid nitrogen as a coolant. Between 100 °C and 150 °C, the maximum cooling rate with the IntraCooler is slightly higher than with liquid nitrogen cooling. Table 2 summarizes the advantages and disadvantages of the various cooling options. The measuring cell should be purged with about 200 ml/min of dry gas when using the IntraCooler, liquid nitrogen or cryostat cooling options in order to avoid icing of the furnace.

Cooling option	Minimum Temperature	Advantages	Disadvantages
Air cooling	Room temperature	No additional cooling unit required, no costs involved	Low cooling rates, limited temperature range
Cryostat	variable, depending on the coolant down to −50 °C)	Variable end temperature from time to time	Coolant must be checked from time to time
IntraCooler	> -60 °C	Easy to use, good value	Cools continuously (can be switched off with the power switch
Liquid nitrogen	> -150 °C	Highest cooling rates	Requires liquid nitrogen, complexity

Table 2. Summary of the different DSC821e.cooling options

Exhibitions, Conferences and Seminars - Veranstaltungen, Konferenzen und Seminare

6th Laehnwitzseminar on Calorimetry	June 13-17, 2000	Kuehlungsborn (Germany)
AIMAT	17-21 Luglio 2000	Spoleto (Italy)
ICTAC 2000	August 14-18, 2000	Copenhagen (Denmark)
PhandTA5, 5th Sympoisum on Pharmacy and TA	September 19-21,2000	Basel (Switzerland)
25 Years STK	September 21-22,2000	Basel (Switzerland)
NATAS	October 4-8	Orlando (USA)
Tentoonstelling "Het Instrument" van	9 – 14 Oktober 2000	Utrecht (Netherlands)
AICAT	13-16 Dicembre 2000	Camogli (Italy)

TA Customer Courses / Seminars in Switzerland - Information and Course Registration:
TA Kundenkurse / Seminare in der Schweiz - Auskunft und Anmeldung bei:

Helga Judex, METTLER TOLEDO GmbH, Schwerzenbach, Tel.: ++41-1 806 72 65, Fax: ++41-1 806 72 40, e-mail: helga.judex@mt.com

TMA/DMA (Deutsch)	11. September 2000	Greifensee	TMA/DMA (English)	September 18, 2000	Greifensee
STARe SW Workshop Basic (D)	11. September 2000	Greifensee	STARe SW Workshop Basic (E)	September 18, 2000	Greifensee
TGA (Deutsch)	12. September 2000	Greifensee	TGA (English)	September 19, 2000	Greifensee
DSC Basic (Deutsch)	13. September 2000	Greifensee	DSC Basic (English)	September 20, 2000	Greifensee
DSC Advanced (Deutsch)	14. September 2000	Greifensee	DSC Advanced (English)	September 21, 2000	Greifensee
STARe SW Workshop Adv. (D)	15. September 2000	Greifensee	STARe SW Workshop Adv. (E)	September 22, 2000	Greifensee

Workshop Tips und Hinweise für gute Messungen	20. November 2000	Greifensee
Workshop Kurveninterpretation	21. November 2000	Greifensee
Seminar Kopplungstechniken	22. November 2000	Greifensee
Seminar Dynamisch Mechanische Analyse (DMA)	23. November 2000	Greifensee

TA-Kundenkurse und Seminare (Deutschland)

Für nähere Informationen wenden Sie sich bitte an METTLER TOLEDO GmbH, Giessen: Frau Ina Wolf, Tel.: ++49-641 507 404.

DSC-Kundenkurs	7./8.11. 2000	Giessen/D
TG-Kundenkurs	9./10.11. 2000	Giessen/D
Fachseminar: Thermische Analyse an polymeren Werkstoffen in der Automobilindustrie	28.9. 2000	Giessen/D
DMA-Messtechnik – die Methode und ihre Anwendungen	29.9. 2000	Giessen/D

Cours et séminaires d'Analyse Thermique en France et en Belgique

France: Renseignements et inscriptions par Christine Fauvarque, METTLER TOLEDO S.A., Viroflay,

Tél.: ++33-1 30 97 16 89, Fax: ++33-1 30 97 16 60.

Belgique: Renseignements et inscriptions par Pat Hoogeras, N.V. METTLER TOLEDO S.A., Lot,

Tél.: ++32-2 334 02 09, Fax: ++32 2 334 02 10.

TMA (français)	2 Octobre 2000	Viroflay (France)
TGA (français)	3 Octobre 2000	Viroflay (France)
DSC Basic (français)	4 Octobre 2000	Viroflay (France)
DSC Advanced (français)	5 Octobre 2000	Viroflay (France)

Jour d'information	26 Septembre 2000	Mulhouse (France)
Jour d'information	6 Octobre 2000	Paris (France)
Jour d'information	24 Octobre 2000	Paris (France)
Jour d'information	14 Novembre 2000	Montpellier (France)
Jour d'information	28 Novembre 2000	Poitiers (France)

STARe User Forum	18 Octobre 2000	Bruxelles (Belgique)
TA Information Day	19 Octobre 2000	Bruxelles (Belgique)
Cours spécifique sur l'Analyse Thermique de Polymères	8 Novembre 2000	Bruxelles (Belgique)
Specifieke cursus over Thermische Analyse op Polymeren	9 Novembre 2000	Bruxelles (Belgique)

TA Customer Courses and Seminars in the Netherlands

For further information please contact: Hay Berden at METTLER TOLEDO B.V., Tiel, Tel.: ++31 344 63 83 63.

Corsi e Seminari di Analisi Termica per Clienti in Italia

Per ulteriori informazioni prego contattare: Simona Ferrari

METTLER TOLEDO S.p.A., Novate Milanese, Tel.: ++39-2 333 321, Fax: ++39-2 356 2973.

Corsi per Clienti

DSC base	5 Giugno, 18 Settembre 2000	Novate Milanese
DSC avanzato	6 Giugno, 19 Settembre 2000	Novate Milanese
TGA	7 Giugno, 20 Settembre 2000	Novate Milanese
TMA	8 Giugno, 21 Settembre 2000	Novate Milanese

Giornate di informazione

	14 Giugno 2000	Genova

TA Customer Courses and Seminars for Sweden and the Nordic countries

For details of training courses ans seminars please contact:

Catharina Hasselgren at Mettler Toledo AB, Tel: ++46 8 702 50 24, Fax: ++46 8 642 45 62

E-mail: catharina.hasselgren@mt.com

TA Customer Courses and Seminars in USA and Canada

Basic Thermal Analysis Training based upon the S**TA**R^e System version 6 is being offered April 21-22 and October 12-13 at our Columbus, Ohio Headquarters. Training will include lectures and hands-on workshops.

For information contact Jon Foreman at 1-800-638-8537 extension 4687 or by e-mail jon.foreman@mt.com

TA course	June 21 – 22, 2000	Columbus (OH)
TA course	October 10 – 11, 2000	Columbus (OH)

TA Customer Courses and Seminars in UK

For details of training courses and seminars please contact:

Rod Bottom at METTLER TOLEDO Ltd., Leicester, Tel.: ++44-116 234 50 25, Fax: ++44-116 234 50 25.

TA Information Day:

7 June 2000	Warrington
14 June 2000	Bristol

TA Customer Training Courses in the South East Asia regional office, Kuala Lumpur

For information on dates please contact:

Malaysia:	Jackie Tan/Ann Owe	at ++ 603-7032773, fax: 603-7038773
Singapore:	Lim Li/Clive Choo	at ++ 65-7786779, fax: 65-7786639
Thailand:	Warangkana/Ajjima Sartra	at ++ 662-7196480, fax: 662-7196479
Or SEA regional office:	Soosay P.	at ++ 603-7041773, fax: 603-7031772

For further information regarding meetings, products or applications please contact your local METTLER TOLEDO representative.

Bei Fragen zu weiteren Tagungen, den Produkten oder Applikationen wenden Sie sich bitte an Ihre lokale METTLER TOLEDO Vertretung.

Internet: http:/www.mt.com

METTLER TOLEDO